Event-related Potential Measurements of Long-term Orientation-specific Contrast Adaptation

A Dissertation

SUBMITTED TO THE FACULTY OF

UNIVERSITY OF MINNESOTA

BY

Yihwa Baek

IN PARTIAL FULFILLMENT OF THE REQUIREMENTS

FOR THE DEGREE OF

DOCTOR OF PHILOSOPHY

Stephen A. Engel, Ph.D.

October 2019

Acknowledgements

I would like to express sincere gratitude to my advisor Dr. Stephen Engel for his valuable guidance, patient support and constant encouragement in the long journey. I would also like to thank the other members of my dissertation committee, Dr. Gordon Legge, Dr. Daniel Kersten, and Dr. Nathaniel Helwig for helpful comments and inspiring questions.

My gratitude also goes to all of the previous and current Engel lab members and other CAB area colleagues for interesting discussions in and out of the lab. I would also like to appreciate the undergraduate RAs for their time and effort put in my experiment.

I would like to thank all my friends around the globe, for spending time with me, making me laugh, and helping me go through hard times. Special thanks go to Liz Fast and Hyun Euh who are my family in Minnesota.

Finally, I am deeply thankful to my family, for their unconditional love, support, and encouragement.

Abstract

The visual system continuously adjusts how it responds to current stimulus based on the history of the incoming stimuli, a process referred to as visual adaptation. Most of the previous studies focused on short-term adaptation effects ranging from milliseconds to minutes. Recent work has showed behavioral effects of long-term adaptation (hours and days), but their neural mechanisms remain unexplored.

We aimed to uncover the neural bases of long-term orientation-specific contrast adaptation in an electroencephalography (EEG) experiment. Subjects were deprived of vertical contrast for 4 hours using altered reality goggles, which filtered out vertical energy from the scene in real-time. Event-related potentials (ERPs) in response to vertical and horizontal gratings were recorded before and after the long-term deprivation. We hypothesized that ERP response to vertical stimulation would increase in strength, and might decrease in latency, after the long-term deprivation. Results were analyzed by computing simple amplitudes of response, by comparing model fits to the ERP time courses, and by using the spatial pattern of ERP responses to classify trials by stimulation type.

Early ERP components in response to vertical increased in amplitude and decreased in latency following adaptation, relative to responses to horizontal, but these differences were not significant. However, model fitting and classification results both revealed significantly greater differences in ERP responses between vertical and horizontal stimulation following adaptation. Collectively, these results suggest that long-term adaptation changes the amplitude of response in early visual cortex.

Table of Contents

List of Tables

List of Figures

Chapter 1

Chapter 2

Chapter 1. Background and Motivation

Can the adult early visual cortex rewire itself? The answer to this is important for both basic science research and for translational applications. If reliable methods could be found to produce controlled plasticity in adults, then new therapies taking advantage of these methods could improve visual function in patients with visual impairments, such as amblyopia or macular degeneration.

There are a number of ways for producing plasticity in adult visual cortex, including perceptual learning (for reviews, Fahle, 2005; Fine & Jacobs, 2002; Goldstone, 1998; Huxlin, 2008; Sagi, 2011; Seitz & Dinse, 2007), and rejuvenating cortex to put it a more plastic state (e.g. Villeda et al., 2014; Wyss-Coray, 2016). These methods are receiving large amounts of attention in the field because of the above-mentioned clinical implications.

Recently, however, long-term adaptation has been proposed as a method for generating long-term plasticity in adult cortex (e.g. Bao & Engel, 2019). Here we test whether these methods can indeed produce changes in or around primary visual cortex.

We first review adaptation generally to give a sense of what is and how it works. We then discuss the time course of build-up and decay of adaptation, because our goal is to make it last a long time. Finally, we talk about previous work trying to induce long-lasting plasticity by using long-term adaptation.

1.1 Contrast Adaptation

Visual adaptation can be defined as altered neural and perceptual responses due to exposure to a preceding visual stimulus (Blakemore & Campbell, 1969; Clifford et al., 2007; Kohn, 2007; Krekelberg, Boynton & van Wezel, 2006; Larsson, Solomon & Kohn, 2016; Solomon & Kohn, 2014). Many aspects of a preceding visual stimulus, such as its contrast, spatial frequency, color, shape and motion, elicit adaptation resulting in altered perception of the corresponding feature of the following stimulus.

Contrast adaptation occurs when neurons in the visual system change their properties following exposure to a stimulus of particular contrast. For example, adaptation to a high contrast grating makes the neural response to the contrast of a subsequent, similar stimulus weaker (Campbell & Maffei, 1970; Heinrich & Bach, 2002a; 2002b; Nelson et al., 1984).

Contrast adaptation also changes how we perceive a stimulus (Figure 1). After the presentation of a high contrast grating, the contrast of the following stimulus looks lower contrast than before adaptation (Blakemore & Campbell, 1969; Hammett, Snowden & Smith, 1994). Most accounts of adaptation propose that it is beneficial, allowing the visual system to function better as the visual environment changes.

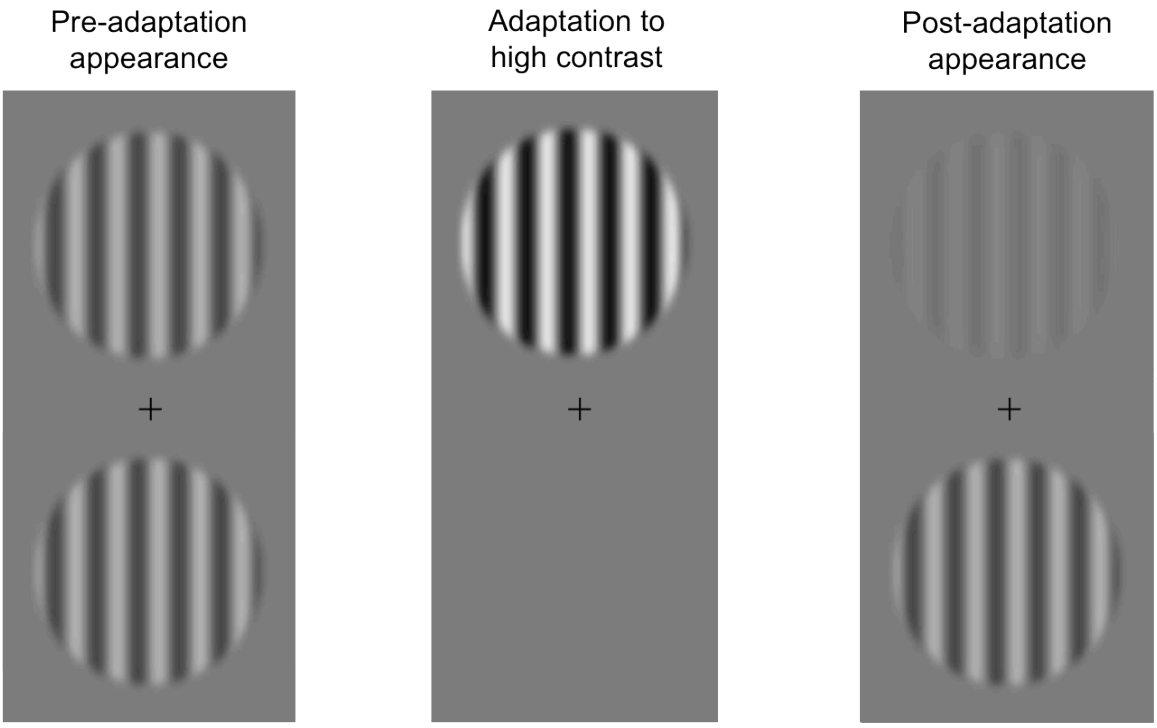

Figure 1. A schematic example of contrast adaptation. After adaptation to a high contrast sine grating in the upper visual field, the apparent contrast is lower at the adapted site.

Historically, research on visual adaptation was used as a method to study the selectivity of visual processes represented in different channels (reviewed in Webster, 2011). Information regarding visual features, such as orientation, contrast, spatial frequency, shape, color, and motion, are conveyed through visual pathways from the retina to the lateral geniculate nucleus (LGN) to higher visual areas in the brain. If there are sets of neurons that respond selectively to the property of a certain feature, presenting a visual stimulus with that property can elicit selective adaptation of those neurons. For example, if there is a set of neurons that responds to a vertical orientation, a visual stimulus with vertical orientation will evoke neural activity in those vertical-selective neurons more than other neurons. The subsequent percept of oriented stimuli will be influenced by this

selective response such that the apparent contrast of vertical patterns will be reduced while that of horizontal ones will be unaffected.

More recently, attempts have been made to understand how adaptation is functionally important for observers in and of itself. One of the proposed functional benefits of adaptation is that it makes neural coding more efficient (Kohn, 2007; Solomon & Kohn, 2014; Wainwright, 1999; Webster, 2012). Efficient codes get the most information out of neurons with limited dynamic range (Barlow, 1990). A way adaptation may increase efficiency is by reducing the redundancy of the coding, which in turn will produce metabolic savings (e.g. Srinivasan, Laughlin & Dubs, 1982).

Another potential benefit of adaptation is to enhance the saliency of unexpected information. Adaptation can help the visual system to be more responsive to novel stimuli (Dragoi, Sharma & Sur, 2000; Sharpee et al., 2006). A final suggested functional benefit of adaptation is improved discriminability of the stimuli around the adapter (Abbonizio, Langley, & Clifford, 2002; Greenlee & Heitger, 1988). However, the link among single cell tuning, population coding and psychophysical performance is not clear enough yet to determine if adaptation can improve discriminability (Solomon & Kohn, 2014; Webster, 2012). In part to help resolve this debate, and in part simply because its effects are so large and pervasive, current research on adaptation attempts to understand how and where adaptive changes take place in the visual system.

1.1.1 Basic Measurements of adaptation

1.1.1.1 Psychophysical Measures

Many different psychophysical tasks have been used to measure effects of adaptation in the laboratory. All adaptation experiments have distinct adapting and testing phases. In the adaptation phase, contrast adaptation can be elicited by prolonged exposure to a high contrast stimulus, such as sine wave grating.

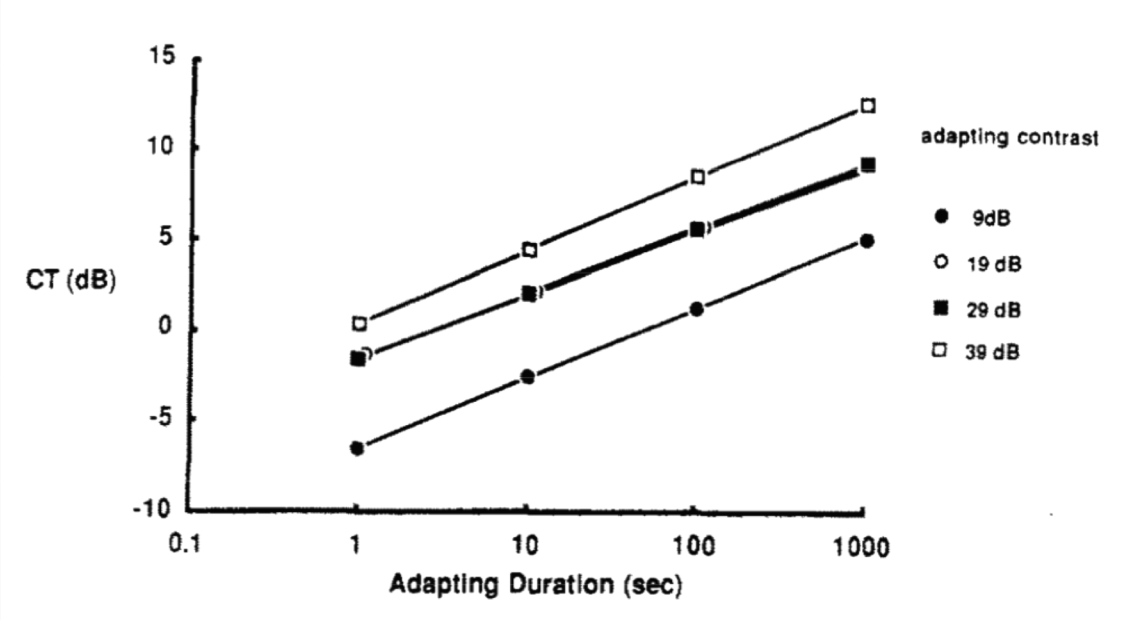

Figure 2. Contrast threshold (CT) as a function of adapting duration. Threshold elevation is higher with longer duration and higher adapting contrast. Reprinted from Greenlee et al. (1991).

Many different psychophysical tests reveal adaptation effects. One of the basic behavioral measurements of contrast adaptation is measuring detection thresholds (Greenlee et al., 1991; Magnussen & Greenlee, 1985; 1986; Pavan, Marotti & Campana, 2012). In a contrast detection task, subject is exposed to a high contrast stimulus for a certain amount of time. Once the adapter is removed, test stimulus with low contrast near the threshold is presented. Looking at high contrast adapter causes the appearance of the test to be lower contrast than its veridical contrast. So, the contrast necessary to be detected is higher than the original detection threshold. This threshold

elevation (TE) in the test stimulus caused by adapting stimulus is one of the widely used methods of measuring contrast adaptation psychophysically (Figure 2). The effect of adaptation in detection threshold is known to be orientation and spatial frequency selective (Blakemore & Campbell, 1969; Foley & Boynton, 1993; Legge & Foley, 1980; Stecher, Sigel, & Lange, 1973).

The tilt after-effect (TAE) is another way to measure orientation specific contrast adaptation (Magnussen & Johnsen, 1986). After adaptation to a tilted orientation, the perceived orientation of subsequent stimuli is shifted from the orientation of the adapter. For example, after adapting to a high contrast and 30 degree clockwise-tilted grating, a vertical grating following the adapter appears tilted counterclockwise, away from the adapter's orientation. The amount of clockwise adjustment needed to make the grating look vertical is the size of the adaptation effect. The TAE is thought to occur because exposure to the adapter selectively reduces the gain of neurons that are tuned to the 30-degree clockwise orientation, shifting the neural population response function away from 30 degrees.

Another behavioral task to measure adaptation is contrast matching (Hammett et al., 1994; Langley, 2002; Ross & Speed, 1996). This method is used to estimate the apparent contrast of a test stimulus after adaptation by comparing it to another stimulus with "standard" contrast. For example, after adapting to a high contrast grating on one side of the display, a test stimulus with fixed contrast is presented on the adapted side and a standard stimulus is simultaneously presented on the unadapted side of the display. The subject's task is to decide which one of the two gratings appears to have higher contrast. If the perceived contrast of the standard grating is higher, its contrast is

lowered in the next trial and vice versa until the contrasts of two gratings match. Alternatively, the standard grating is presented with random contrasts in many trials. In either case, the equivalent contrast of the perceived contrast of the test grating can be found as the 50% point on a psychometric function relating the side picked to the test contrast.

1.1.1.2 Neurophysiological Measures of Adaptation in Humans

In humans, adaptation effects can be measured electrophysiologically with the electroencephalogram (EEG). Visually evoked potentials (VEPs) are electrical signals elicited by visual stimuli and recorded from the scalp. VEPs are thought to index activity in early visual cortex, since their amplitude scales with stimulus contrast (Campbell & Maffei, 1970).

Contrast adaptation changes the amplitude of the VEP (Heinrich & Bach, 2001; Mecacci & Spinelli, 1976), but its latency is not largely affected (Heinrich & Bach, 2001). Some studies showed decreased VEP after adaptation to high contrast (Mecacci & Spinelli, 1976; Nelson et al., 1984; Suter et al., 1991; Figure 3), but others reported increased VEP with adaptation (Bach, Greenlee & Bühler, 1988; Rebaï & Bonnet, 1989). Heinrich and Bach (2001; 2002a; 2002b) observed both increased and decreased VEP depending on the contrasts of adapting and test stimuli, and also depending on whether the adapter and test stimulus have matching spatial frequency or temporal frequency.

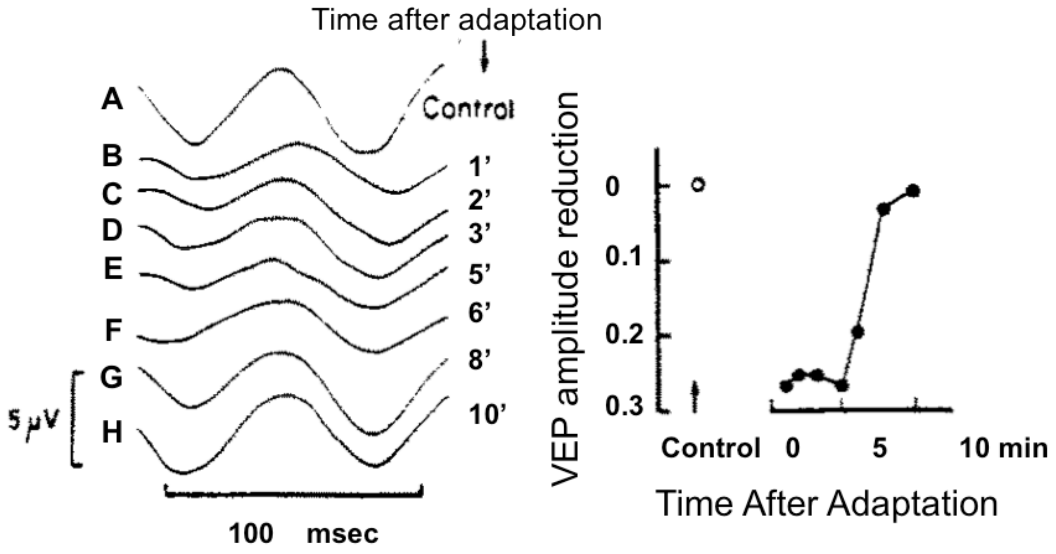

Figure 3. Effect of adaptation to 40% contrast on VEP amplitude. Test contrast was 8%. (Left) B-H are VEPs 1-10 minutes after adaptation. (Right) VEP amplitude reduction holds up to 5 minutes (B-E) after adaptation. Adapted from Mecacci & Spinelli (1965).

Suter and colleagues (1991) suggested that there are several critical variables that determine whether adaptation will produce VEP attenuation. Most intuitively, attenuation should be seen in conditions that maximize behaviorally observed adaptation, which include high contrast adapters and low contrast tests. For example, Bach and colleagues (1988) found a decrease in VEP amplitudes when test contrast was below 7%, but increased VEP amplitudes with test contrast above 7%. This account also explains the results of Rebaï and Bonnet (1989), who observed enhanced VEP using a 60% contrast adapter and test.

A possible explanation for observing enhanced VEP, when test and adapter differ in spatial frequency, is the interaction between spatial-frequency (SF) tuned channels (Suter et al., 1991). If different SF channels inhibit each other, then adaptation can elicit VEP amplitude facilitation at a spatial frequency distant from the adapter SF. This is

because adaptation lowers the response at the adapter's SF channel, which in turn releases the test SF channel from inhibition. Prior VEP evidence using masking has demonstrated the existence of mutual inhibition between stimuli at different spatial frequencies, adding to the plausibility of this account (Fiorentini, Pirchio, & Spinelli, 1983; Regan, 1983). This account is also consistent with a psychophysical finding that the effect of adaptation from an adapter containing components at two SFs is greater when the SFs are similar, and smaller when the SFs differ by 1.0-2.0 octaves (Greenlee & Magnussen, 1988).

Functional magnetic resonance imaging (fMRI), that measures changes in blood-oxygen-level-dependent (BOLD) signal, is another way to measure adaptation in humans physiologically (Krekelberg et al., 2006). Repeated or prolonged exposure to a stimulus reduces the BOLD signal from the following stimulus (Grill-Spector, Henson, & Martin, 2006). Gardner and colleagues (2005) showed that higher stimulus contrast leads to higher BOLD signal in visual brain areas, and that adaptation to higher contrast stimuli shifts the contrast-response functions (CRFs) to the right in V1-V3. This rightward shift of CRF indicates an overall decrease in the contrast gain in all contrast levels following adaptation. They also observed the centers of the CRFs (C_{50}) were positioned closely to the adapted contrast level (Figure 4).

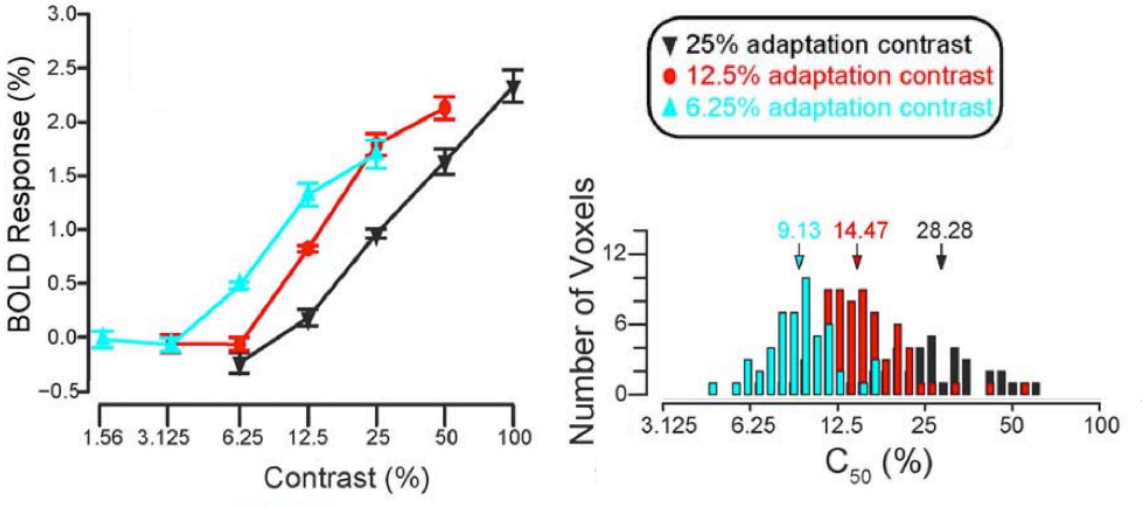

Figure 4. BOLD response to checkerboard plaids after adaptation. Reprinted from Gardner et al. (2005).

The orientation selectivity of neurons in human visual areas has been investigated using contrast adaptation and fMRI. Effects of adaptation on the BOLD signal were compared when the test stimulus had the same property as adapter and when the test stimulus differed from the adapter. Bigger effects of adaptation for the test stimulus similar to the adapter, indicates adaptation of a neural population selectively responsive to the adapter property.

Several studies have used this approach to demonstrate orientation selectivity (Boynton & Finney, 2003; Fang et al., 2005; Larsson, Landy, & Heeger, 2006; Tootell et al., 1988). For example, Larsson and colleagues (2006) found stronger response to the probe whose orientation was orthogonal to the adapted orientation than to a probe parallel to the adapter in V1. This result indicates that the parallel orientation was more influenced by the adaptation than the orthogonal orientation.

Contrast adaptation and fMRI have also been used to elucidate where specific visual processes originate in cortex. Larsson and Harrison (2015) distinguished inherited vs. intrinsic adaptation in higher visual areas by comparing their spatial specificity of adaptation to that of V1. They found spatial specificity of adaptation in higher visual areas to be similar as in V1. This result indicates that the adaptation effect measured in the higher areas is likely to be inherited from V1, not originating in that area, since later areas should have bigger receptive fields, resulting in less spatial specificity.

Montaser-Kouhsari and colleagues (2007) measured fMRI responses in early and higher visual areas to illusory contours, by adapting subjects to illusory contour induced by short line segments. They found orientation selectivity of adaptation in higher areas as well as in early areas, and claimed that both early and higher areas have neurons that respond selectively to the orientation of the illusory contour. However, the selectivity observed in higher areas might be inherited from earlier areas (Larsson & Harrison, 2015).

Bi et al. (2009) employed orientation selective adaptation to find the locus of crowding, which is difficulty in identifying a peripheral target stimulus in the presence of nearby flanking stimuli. They tested if crowding influences adaptation in V1-3. The adapting stimulus (a tilted grating) was presented either with or without flankers, and the adaptation effect was measured as difference of BOLD signal change between orthogonal and parallel test stimuli. If crowding affected adaptation, there would have been less signal change with flankers because crowding would have weakened the response to the adapter. Such an influence of crowding on adaptation was not found in V1, but was found in V2 and V3, indicating that crowding occurs beyond V1.

1.2 Time Course of Adaptation

1.2.1 Functional Form

The temporal aspect of adaptation is worth studying because adaptation is closely related to ‘time’ by definition, in that the preceding stimulus results in change of the response to the subsequent stimulus. The change in preceding stimulus can be as short as several milliseconds or it can be very slow, taking several hours. Thus, it may be helpful to pool the studies using wide range of time scales in various levels of visual processing to better understand adaptation.

The two curves in Figure 5 characterize the time course of adaptation. As exposure to the adapter increases, the amount of adaptation rises; the function relating these two quantities will be called the build-up curve (Figure 5). When the adapter is removed, the amount of adaptation decreases over time following a function called the decay curve (Figure 5). The build-up curve has a typical shape; when plotted on linear axes adaptation grows quickly at first and then grows more slowly over time. Decay curves also are steeper at their beginning and become shallower over time when plotted on linear axes.

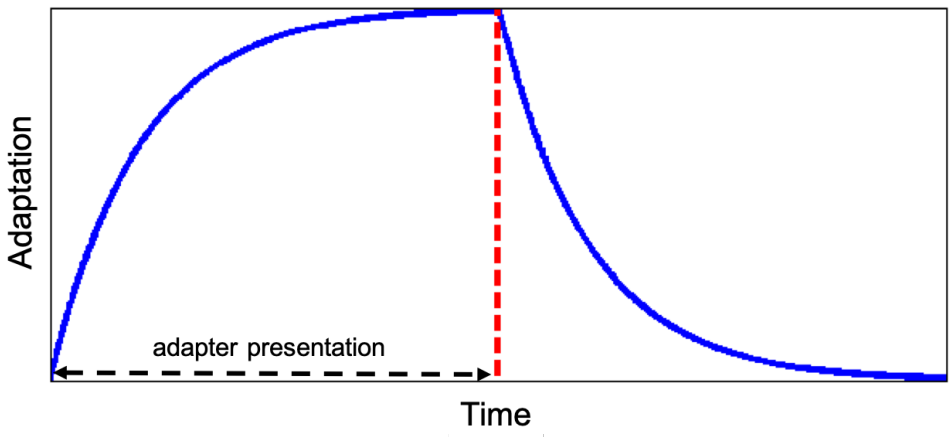

Figure 5. Time course of adaptation. Build-up of adaptation effect as a function of adapter presentation duration, and decay of adaptation effect after offset of the adapter.

Both build-up and decay curves have been characterized as exponential and power functions. For the exponential form, the build-up of the adaptation effect E as a function of time t is expressed as: $E(t) = S - a * e^{-rt}$, where S is a horizontal asymptote and r is the growth rate. For the power function form, the build-up can be expressed as $E(t) = a * t^p$, where *a* is a scaling factor and p, generally less than 1, determines the overall shape of the curve. In the log-log plot, a power function is linear, with p as the slope and a as the intercept of the line.

Similarly, for the decay curve, the exponential form of the function can be expressed as $E(t) = I * e^{-rt}$, where I is the initial point of adaptation effect where the decay starts, and r is the decay rate, or equivalently as $E(t) = I * e^{-t/\tau}$, where τ is a time constant. τ is the time that takes to decay until it reaches to $I * e^{-1}$ or about 37% of the initial value. For the power function form, the decay curve is $E(t) = S - a * t^p$, where S is the adaptation effect at the beginning of the decay period.

A number of papers have fit both exponential and power functions to adaptation data. Several that did this test for the decay curve found a better fit for exponential function (Foley & Boynton, 1993; Pavan, Marotti & Campana, 2012; Patterson, Wissig & Kohn, 2013), but others found power functions to fit better for both build-up and decay curves (Dong, Engel, & Bao, 2014; Drew & Abbott, 2006).

Power functions can result from multiple exponential processes with different time scales (Drew & Abbott, 2006). It is likely that longer adaptation is fitted better with multiple exponential functions or a power function than a single exponential function, since more processes may become involved over time. Exponential functions are more likely for short duration, and so fit the results of many single cell studies (which used shorter durations; Albrecht, Farrar, & Hamilton, 1984; Carandini & Ferster, 1997; Descalzo et al., 2005; Duong & Freeman, 2007; Patterson, Wissig, & Kohn, 2013; Wark, Fairhall, & Rieke, 2009). Papers that used power function to fit the adaptation effect tend to be psychophysical studies, where longer durations are common (Bao & Engel, 2012; Dong, Engel, & Bao, 2014; Greenlee et al., 1991; Magnussen & Greenlee, 1985; 1986; Snippe & Hateren, 2003). In addition, power functions in psychophysical studies may arise because data are sometimes averaged across many observers.

1.2.2 Strength of Build-up

What factors make adaptation stronger or weaker, or make it last a longer or shorter duration? This question is of interest because it may lead to methods to make beneficial adaptation particularly strong or long-lasting, or methods to make harmful adaptation weaker or shorter-lasting. Many different factors affect the shape of the build-up and decay curves. These include the duration of adaptation, the strength of the adapting

stimulus, the similarity between adapter and test, and the spacing of the adapting duration.

The asymptote of the adaptation curve corresponds to the maximum of the measurable adaptation effect. Adapting contrast is one of the variables that influence how far the adaptation effect can grow. Maximum threshold elevation was larger for higher adapting contrast (Blakemore & Campbell, 1969). However, in Nelson et al. (1984) where VEP was measured, the dependence of the maximum adaptation effect on adapting contrast did not hold beyond 20% contrast. Maximum adaptation was reached with 20% contrast, and higher contrast beyond that did not elicit further adaptation.

However, the time required to reach asymptotic adaptation appears to vary across the method of measurement and the stimuli used. In a single cell study, decreased response after adaptation to 80% contrast moving grating reached asymptote after only 10-20 seconds (Sclar, Lennie, & DePriest, 1989). In an EEG study, evoked potential amplitude reached asymptote after 15 minutes adaptation to 40% contrast grating (Mecacci & Spinelli, 1976). In a behavioral study involving 3-hour adaptation to 60% adapter, asymptotic effects were not reached until 30 to 60 minutes of adaptation for two subjects (Magnussen & Greenlee, 1985), though the threshold was measured every 10-30 minutes.

One factor complicating interpretation of build-up functions is that some decay will necessarily have occurred in between the end of adaptation and the first measurement of its effects. Foley and Boynton (1993) pointed out that this temporal gap between the offset of the adapter and subsequent measurements makes it difficult to distinguish

between the amount of adaptation and the rate after recovery. They claimed that less than 100 ms is required for a maximum effect of adaptation, and that build-up functions may simply reflect slower and slower decay as adaptation lengthens (see below). Some of the variability in the studies above that measured the amount of time required to reach asymptotic adaptation may thus be due to differences in the temporal gap between the adapter and the stimulus used to measure adaptation.

1.2.3 Rate of Decay

The shape of the decay curve is also influenced by several factors. The time required for complete decay of adaptation effect depends on adapting duration (Pavan et al., 2012). With longer adapting duration, it needs more time to recover to the initial level of response before adaptation (Blakemore & Campbell, 1969).

However, the adapting duration does not influence on the rate of decay that is shown as the *slope* of the decay function on log-log axis. Magnussen and Greenlee (1985) observed that the slope of the decay functions after 2- and 10-minutes adaptation remained the same as in 3-hour adaptation. The same slope on the log-log axis mean it follows the power function with the same power, only differing the intercept that is a multiplicative constant on the linear axes (Greenlee et al., 1991). Instead, the slope of the decay function depends on the contrast of adapting stimulus (Blakemore & Campbell, 1969; Pavan et al., 2012).

The shape of the decay function is also influenced by whether the adaptation was continuous or interrupted. Magnussen and Greenlee (1986) compared five 2-minutes adaptation varying inter-adaptation interval (IAI) 0-180 seconds with continuous 10

minutes adaptation. IAI longer than 60 seconds showed difference from continuous adaptation. This result indicates the possibility of two-process model where the first stage recovers fast, and the second stage recovers slower and controls decay rate. Boynton and Finney (2003) found similar results using fMRI. Two gratings either with the same orientation or orthogonal orientations presented varying stimulus onset asynchrony (SOA; 1.125-8 seconds). They found reduced BOLD signal and delayed time course in the orthogonal conditions with short SOA, but the difference became smaller with longer SOA.

1.3 Long-term Contrast Adaptation

How strong can contrast adaptation become in the limit, and how long can it last? The answers to these questions are important because if adaptation can produce large semi-permanent changes in early visual cortex, then it may be applicable to the treatment of visual disorders.

To answer these questions, our lab developed methods to induce contrast adaptation over long durations. Subjects wore a pair of altered reality (AR) goggles, which digitally adjusts specific visual features from a head-mounted camera and feed them to subjects. It enables subjects to see the real environment they are in through the camera while they do everyday activities, which allows them to stay in the adapting environment for a long duration. It also has the advantage of inducing the demands of the plasticity of the visual system because it promotes interaction with the environment, rather than simply sitting in front of a computer display.

Because the method operates on natural images, it is more convenient to reduce the contrast of a particular orientation than it is to enhance it. Because a given orientation is only present intermittently in any natural image, removing it can essentially guarantee adaptation to zero contrast, while enhancing it will produce adaptation to a contrast that varies to some extent with the content of the input images.

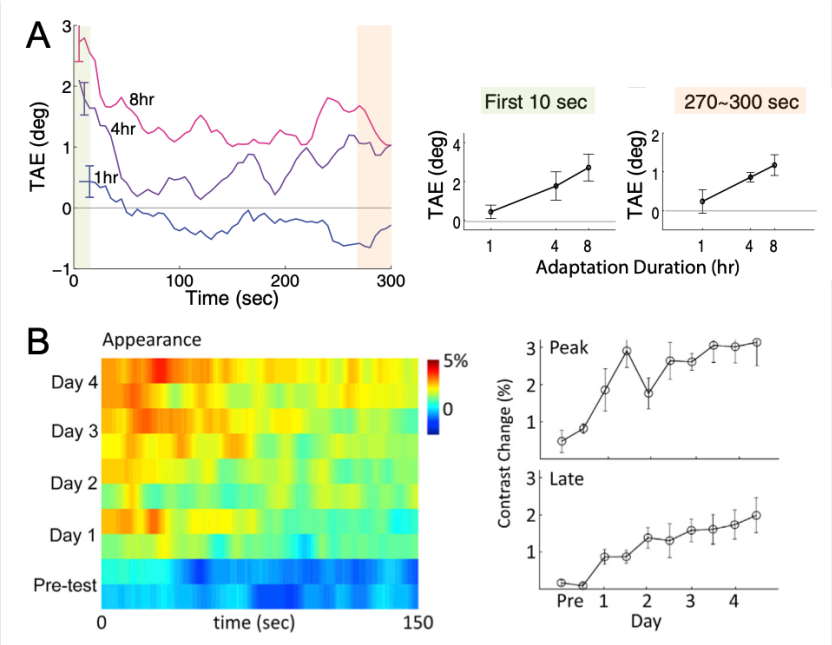

Figure 6. Previous studies on long-term adaptation. (A) Tilt after-effect measured after 1, 4, and 8 hours of deprivation (Bao & Engel, 2012). (B) Change in apparent contrast measured by contrast matching for 4 days (Haak et al., 2014). Left panel colors depict the extent of change as a function of time during test sessions. Right panel plots the maximum change (top), and the ending level (bottom) of each testing session (2 sessions per day). Figures adapted from the original papers.

Past work from the lab using these methods shows that contrast adaptation continues to grow over long durations, even up to 4 days. Zhang et al. (2009). measured contrast threshold after 4 hours of adaptation to removal of vertical contrast, using the AR goggles. Contrast detection thresholds decreased for the adapted orientation, indicating increased responsiveness of the neurons selective for the deprived orientation after adaptation. Bao and Engel (2012) measured TAE before and after deprivation and found

that the effect of contrast deprivation grew with the duration of adaptation, up to 8 hours (Figure 6A). Haak et al. (2014) extended the duration of adaption even further, up to 4 days of deprivation (Figure 6B).

An interesting result from Haak et al. (2014) was that the effect of adaptation shows two different patterns. The peak adaptation effect of each day was the largest following the first day of adaptation (Figure 6B, top right), whereas the ending level of each day kept growing slowly over 4 days (Figure 6B, bottom right). This result implies that two different mechanisms operate over short- and long-term adaptation.

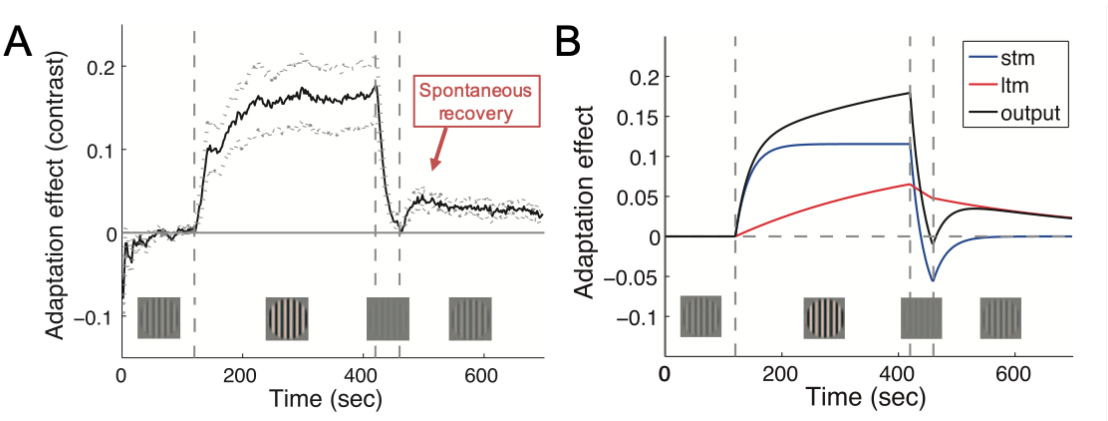

Figure 7. Multiple mechanisms of adaptation (Bao et al., 2013). (A) Time course of adaptation effect from contrast matching experiment. Dashed vertical lines separate baseline, adaptation, de-adaptation, and post-test phases. The contrast of the adapting gratings of each phase was 25%, 80%, 6.25%, and 25%, respectively, and the contrast of the test gratings at un-adapted location was held to 25%. (B) Time course of adaptation effects predicted by two mechanisms with different time constants. A short-term mechanism (stm) which builds up and decays rapidly, and a long-term mechanism (ltm) which grows and decays slower, explain the observed spontaneous recovery of the post-test phase. Adapted from Bao et al. (2013).

Results from Bao et al. (2013), which showed spontaneous recovery of the adaptation effect after de-adaptation, also supported the idea of different mechanisms operating over different time scales. Spontaneous recovery was measured as the lingering effect

of the initial high-contrast adapter, even after the adaptation effect was first canceled by the ‘de-adaptation’ from the low-contrast adapter (Figure 7A). Their work suggests that contrast adaptation is controlled by multiple mechanisms of adaptation in different timescales, and there is a distinct mechanism for long-term adaptation (Figure 7B).

Change of the contrast in natural visual scenes can vary over a wide range of time scales, from transient changes due to saccades or head position, to semi-permanent effects of astigmatism or aging. Many important questions remain about how the visual system adjusts to changes on these many different timescales. Some of them include whether there is a continuum mechanism that control adaptation over different timescales, or whether there are several discrete ones. It is also unclear how the visual system decides whether a given change in the environment is transient or long-term. Finally, it is unknown whether different adaptation effects arise from the same locus in the brain, or whether short- and long-term adaptation have different neural sources.

In general, the mechanism of adaptation that lasts for hours or more has not been explored as much as shorter-term adaptation. In the next chapter, we start trying to fill this gap by answering the question: How does long-term adaptation change neural activity in early visual areas?

Chapter 2. Experiment

2.1 Overview

2.1.1 Research Question

Previous work, reviewed above, showed that longer adaptation durations produce longer-lasting effects (Bao & Engel, 2012; Haak et al., 2014; Zhang et al., 2009). Past work also showed that there is mechanism for long-term adaptation that is distinct from short-term mechanism from psychophysical experiments (Bao et al., 2013). However, the neural bases of long-term contrast adaptation effects are largely unknown. An fMRI study (Kwon et al., 2009) measured the effect of long-term adaptation using a contrast reducing lens. After 4-hour adaptation to a reduced-contrast environment, the contrast discrimination threshold decreased (subjects were able to discriminate smaller difference of stimulus contrasts after adaptation). They also observed increase of BOLD responses in V1 and V2 areas. This result suggests response gain after deprivation. However, the contrast reduction in this study was not orientation specific, so it could have been inherited from changes in the retina or LGN. Orientation specific effects must be cortical, and so could involve a different mechanism.

Our study aimed to find neural evidence for long-term contrast adaptation. We specifically hypothesized that long-term deprivation would enhance responses to the deprived orientation in early visual areas. To test hypothesis, we adapted subjects to vertically-deprived visual scenes using AR goggles for a long duration (4 hrs) to produce long-lasting effect and measured brain activity before and after adaptation.

We measured brain signals with EEG to investigate the neural effects long-term adaptation on early visual areas. We used EEG, as opposed to other methods for measuring human neural activity, because it has good temporal resolution which is beneficial to capture a small and quick response that is early in visual processing.

In the current experiment, event related potential (ERP) was analyzed to examine the effect of adaptation. ERP is time-locked voltage change to an 'event' which is a stimulus presentation, and averaged for each experiment condition. ERPs are believed to arise from synchronous activity of the set of neurons that are involved in the same cognitive process. ERPs have components that comes from these cognitive processes, and the ERP waveform appear as a combination of the components.

The ERP component most closely related to our interest was the C1 component, because it is believed to originate in primary visual cortex. C1 is sensitive to basic visual features such as contrast and spatial frequency, and is the first large peak at 80-100 ms after stimulus onset. It is largest at posterior midline sites, near early visual cortex. There is a characteristic flip in polarity of C1 across stimulation in the upper and lower visual fields, hypothesized to result from the folded shape at calcarine fissure in V1 (Butler et al., 1987; Clark, Fan, & Hillyard, 1995; Di Russo et al., 2001; Foxe & Simpson, 2002; Jeffreys & Axford, 1972a; 1972b; Mangun, 1995).

We used the same long-term adaptation methodology as in prior work from our lab. The method was structured to allow observers to adapt for many hours, while still being able to see reasonably well. Observers wore altered reality goggles that received input from a

head mounted camera. The images from the camera were filtered, removing vertically-oriented contrast, and displayed on the goggles in real-time.

For EEG, we recorded responses to test patterns that contained either the deprived orientation (vertical) or a control orientation (horizontal). To minimize the decay of adaptation effect, the test patterns were interleaved by 'top-up' videos, which were movie clips processed by the same filter used for real-time deprivation filtering. Subjects carried out spatial frequency discrimination task on the test patterns, to maintain spatial attention on the location the stimulus was presented.

2.1.2 Hypothesis

If adaptation to deprivation increases the responsiveness of early visual cortex to the deprived orientation, then the C1 component of the ERP should be relatively larger for vertical stimulation (vs horizontal) following adaptation (vs before). Because stronger neural responses may also produce EEG signals that arise earlier in time, it is possible that the C1 component of the vertical ERP will also have a lower latency (relative to horizontal) following adaptation.

2.2 Methods

2.2.1 Participants

Thirty-six paid subjects participated in the experiment, and 28 subjects completed both pre- and post-adaptation tests. Subjects signed informed consent forms and were explained about the possible discomfort from wearing the altered reality goggles for four hours during adaptation with a wet EEG cap underneath the goggles before and after

adaptation. Eight subjects who either experienced discomfort or failed to produce a good signal-to-noise ratio of EEG signal during the pre-adaptation session did not participate in the post-adaptation tests. Procedures were approved by the University of Minnesota Institutional Review Board. Subjects were compensated with $100 for completing the experiment.

2.2.2 Apparatus

The altered reality system was used to filter out vertical orientation and display it to the subject in real-time (Figure 8). A small USB camera (UI-1220-M, Imaging Development Systems GmbH; 752x480 pixels resolution) was attached on the top front part of the head-mounted display (nVisor SX, NVIS Inc.; 1280x1024 pixels resolution). The camera was connected to a laptop (Dell XPS m1730 with dual NVIDIA 8800m GTX GPU) for image acquisition, filtering, and display. The image processing was performed in MATLAB (The MathWorks Inc., Natick, MA) using Image Acquisition and Psychophysics Toolboxes (Brainard, 1997; Pelli, 1997; Kleiner et al., 2007), and controlled by custom software (Zhang et al., 2009). The filtered image from the laptop is fed to the head-mounted display (HMD) control box and displayed on the HMD.

For EEG recording, we used an Asalab electroencephalography system (ANT Neuro, Enschede, The Netherlands) was used with Waveguard caps (Ag/AgCl scalp electrodes; 10-20 system layout).

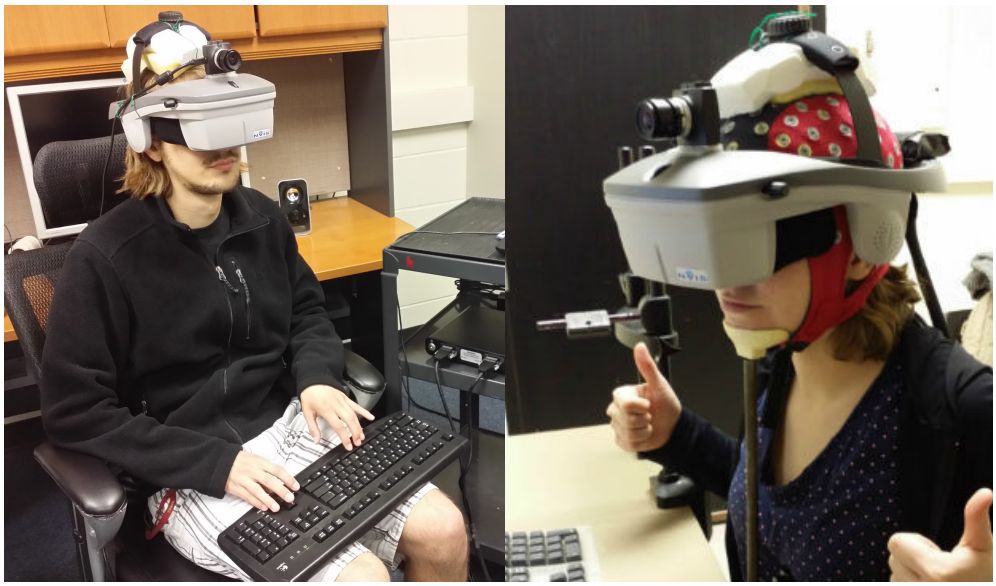

Figure 8. Altered reality system during adaptation (left), and during EEG recording (right).

2.2.3 Stimuli

Adapter filter

The adapting stimulus was video with 85% of vertical energy removed. The video from the camera attached to the HMD was sent to the connected computer for real-time filtering, and the result was fed back to the goggles display subjects wore. Filtering was done by convolving the captured images with a second-order Butterworth filter, and took less than 5 ms, allowing the system to operate in real-time (30 Hz). The amplitude of the Butterworth filter was set to remove 85% of the vertical energy in the images, centered at 1.5 cycles per degree (cpd) and 90° in orientation (vertical). Cut-offs were 0.3 cpd to 7.8 cpd in spatial frequency and 90 ± 37° in orientation; strength fell to less than 2% of maximum outside this range (Figure 9).

Figure 9. An example of original and filtered images.

Filtered images were achromatic, and they seemed blurry due to the removed vertical energy. It was not difficult to recognize most objects in the filtered images especially when motion was present. It was difficult to recognize small objects and small letters in the filtered display. In both cases, there tended to be little information left after filtering of vertical orientation from the original image.

Test gratings

Event-related potentials (ERPs) were measured for circular sinusoidal grating patches. The orientation of the gratings was either vertical or horizontal. The diameter of the patches was 10 visual degrees, and their contrast was 15%. They were presented in either upper (UVF) or lower visual field (LVF), with the nearest edge of the gratings from the display center 0.5° above or below the fixation mark. The spatial frequency of the reference grating was fixed at 2 cpd, and that of the test grating varied from 2 cpd to 3 cpd by 0.0345 cpd steps, in the staircase procedure (see below).

2.2.4 Procedure

The subjects came into the lab on two different days. On the first day, they did pre-adaptation EEG recording as a control condition without adaptation. On the second day, subjects were adapted to the vertically-deprived environment for four hours, and the post-adaptation EEG session followed. EEG recordings of both pre- and post-adaptation took about 46 minutes. The two days were mostly consecutive, but they were allowed to be scheduled several days apart. The post-test was always performed right after adaptation.

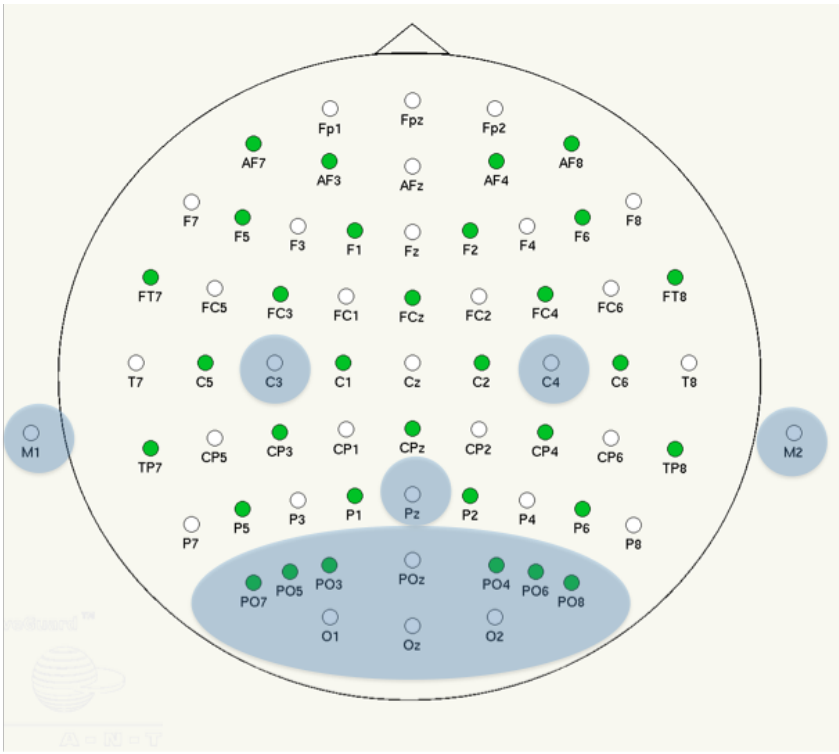

Figure 10. Recording electrode sites. The recorded electrodes are shaded on 10-20 system layout.

Pre- and Post-adaptation EEG recording

EEG was recorded only from the posterior scalp sites as illustrated in Figure 10 (Pz, POz, PO3, PO4, PO5, PO6, PO7, PO8, Oz, O1, O2, C3, and C4). This greatly sped up the cap fitting portion of our already long procedures. The bilateral mastoid electrodes were also recorded to be averaged and used as a reference. The EEG cap was worn beneath the HMD goggles. The EEG signal was digitized at 1024 Hz and resampled offline to 256 Hz.

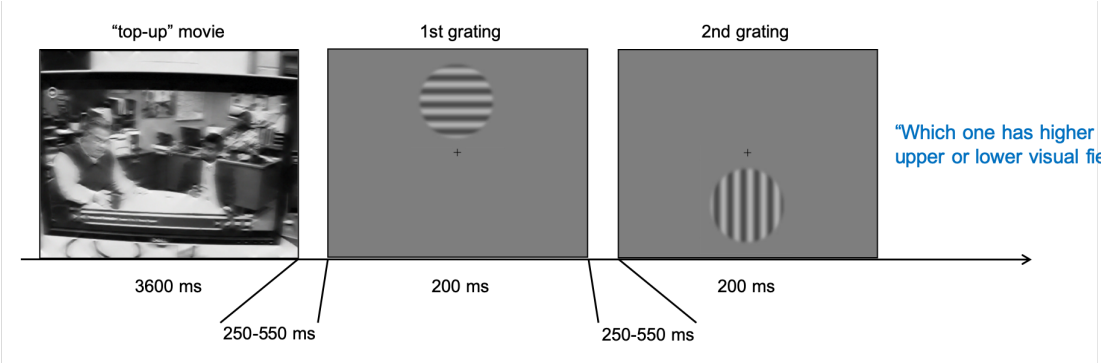

Figure 11. Spatial frequency discrimination task procedure.

Pre- and Post-adaptation tests were about 46 minutes. Each test session consisted of 16 blocks, and each block lasted for 2.9 minutes. Figure 11 depicts a schematic procedure of one trial. Subjects performed 2-alternative forced-choice (2AFC) spatial frequency discrimination task to keep the attention on the stimuli. One vertical grating and one horizontal grating appeared in the upper and lower visual field, temporally separated, with order randomized. After the second grating disappeared, subjects reported which one of the two gratings had higher spatial frequency by pressing up or down arrow button. The duration of test gratings was 200 ms. The second grating was preceded by 250-550 ms blank screen so that there was enough time for the EEG signal from the first grating to return to baseline.

One of the gratings always had 2 cpd spatial frequency as the reference SF, and the SF of the other grating was determined based on the response of the previous trial, using a staircase procedure. It was randomized which one of the upper or lower visual field gratings had the reference SF of each trial. The SF of the test grating started from 3 cpd at the beginning, and 3 correct responses in a row before were required for the staircase to decrease to make the task more difficult. A single incorrect response increased the SF of the test grating to make the task easier. The SF of the test grating increased or decreased by 0.173 cpd after the first trial, and the size of SF increment was reduced to 0.104 and 0.069 after 2 and 5 reversals, respectively, then maintained at 0.035 cpd afterwards. Two staircases were interleaved randomly.

The mean accuracy of the SF discrimination task across subjects was 80.8% as intended in the staircase procedure. The mean spatial frequency of the last 5 trials, averaged across subjects, was 2.15 ± 0.01 cpd which is close to reference SF. There was no significant difference between pre- and post-test performance ($t(13) = 0.44$, $p=.67$). These results confirm that the subjects paid attention to the test gratings during the EEG recording.

Each discrimination trial was interleaved with 3.6 second “top-up” movie clips. Filtered clips were used in the post-adaptation test to maintain adaptation status and to minimize de-adaptation during the test. Non-filtered clips were used in the pre-adaptation test to match the procedures of the post-test. One original video clip was used to make both the filtered and non-filtered videos to keep them consistent other than the filter. The filtered

clips were pre-filtered so that the EEG recording did not involve delay from real-time filtering.

Subjects were instructed to keep their fixation on the center point of the display the whole time. Also, it was emphasized not to blink when the test gratings were on the display, instead to utilize the movie top-up duration for blinking to minimize artifacts in the EEG signal.

4-hour adaptation

During the 4-hour adaptation period, subjects were allowed to do their everyday activities. This encouraged them to view the natural environment, but with vertical orientation filtered out. For convenience, they mainly watched Netflix videos, which are still very rich in visual information. Subjects were instructed not to choose movies that were extreme in certain visual features, such as animated movies or the movies of which scenes are too dark most of the time.

Subjects did different physical activities every hour, for 5 to 10 minutes, both to reduce fatigue from sitting still and to help them experience the adapting images to be the real world. The activities included a beanbag toss, throwing darts, a ring toss, mini basketball, and others.

The first 3 hours of adaptation was done in the lab. During this period, subjects saw the world through the camera. The last hour was done in a separate room where the EEG equipment was housed. In the EEG room, subjects viewed prerecorded filtered video through the goggles, instead of input from the camera.

Transition from adaptation to post-test EEG recording

We set up EEG recording one hour before the test to make the transition from adaptation to testing smooth, minimizing delay between the two phases of the experiment, and so reducing de-adaptation before the test. Subjects adapted for one while wearing the EEG electrodes beneath the goggles, and then proceeded to the post-adaptation test session with only a minimal pause in visual stimulation.

During the move to EEG room, subjects still wore the goggles. Once they got to the EEG room, subjects closed their eyes and the goggles were taken off. Then they were blindfolded while the EEG cap was put on, and then the goggles were repositioned.

2.2.5 Data Pre-processing

EEG data analysis was conducted using the EEGLAB toolbox (Delorme & Makeig, 2004). Only data sets that passed quality control checks were included in the final analyses. Because of the difficult recording conditions, and our requirement that both pre-adaptation and post-adaptation data sets both pass the check, only half the subjects were included in the analysis.

To pass quality control, the data had to meet at least two of the following three criteria: 1) The number of epochs with artifact, as detected by the artifact detection procedure (described below), were less than 20%, 2) ERP topographies from both pre- and post-tests showed evidence of a visible peak of activity near mid-posterior electrodes at around 100 ms post-stimulus (C1), and 3) signals from this peak during upper and lower visual field stimulations showed the characteristic flip in sign, as detected by a peak in

the difference time course (upper-lower) of at least 2 μV. 13, 12, and 10 subjects did not pass each criterion (in order), and 14 subjects did not pass at least two of the criteria, and so were excluded.

Down-sampling & Epoching

Standard ERP preprocessing of the data was conducted. The data were down-sampled to 256Hz offline, and bandpass filtered to 0.1-30Hz using Hamming windowed sinc FIR filter. The down-sampled continuous EEG data were cut into the epochs of the same length for each stimulus presentation event. The length of the epochs was 400 ms, from -100ms to 300 ms around the stimulus onset. For plotting purposes, the baseline was corrected using -200 ms to 0 ms before the stimulus onset by subtracting the mean of this range.

Artifact rejection

To reject epochs that are likely to reflect systematic noise rather than signal, we used the standard artifact detection procedure of EEGLAB. The epochs that had either 1) outlier values of ±30 μV, 2) improbable data outside of 5 s.d. joint probability of electrodes, or 3) strong trends higher than 50μV/epoch were rejected and excluded from analysis. The average number of rejected epochs of the included subjects were 15.53 ± 12.82 % s.d.

Averaging

After artifact rejection, the data were re-referenced to the linked mastoids. The re-referenced epochs of the same conditions were averaged to get an ERP for each condition per subject both in pre- and post-adaptation. By averaging epochs of the same

condition, assumed to show similar patterns, we can compare brain activity across different visual conditions. The set of ERPs for 8 conditions, upper visual field vertical grating (UV), upper visual field horizontal grating (UH), lower visual field vertical grating (LV), and lower visual field horizontal grating (LH) for pre- and post-adaptation, were all computed. Then, all subjects' ERP data were averaged to get grand mean ERP and standard errors across subjects for each condition and session.

2.2.6 Data Analyses

ERPs showed the expected pattern over space and time. Figure 12 shows topographic plots of the grand average data. The voltage topography reveals strong activity around 100 ms in the mid-posterior electrodes, Pz, POz, and Oz, which is positive for stimulation in the lower visual field, and reverses sign for stimulation in the upper visual field. This is expected pattern, and roughly the expected time and location for the C1 component (Butler et al., 1987; Clark et al., 1995; Di Russo et al., 2001; Gomez-Gonzales et al., 1994). Because our hypotheses focus on C1, and because the topography reveals other differences between upper and lower visual field stimulation, many of our analyses will keep data from the two conditions separate.

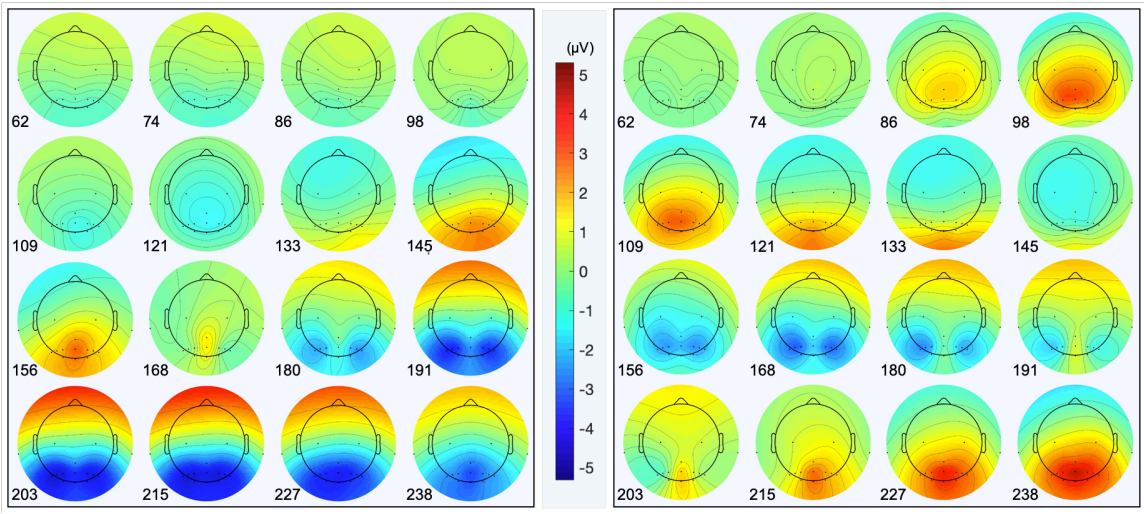

Figure 12. ERP topographies of the grand average collapsing pre- and post-test for the stimulus presented in the upper visual field (left) and lower visual field (right). The number on the lower left corner of each frame indicates time after stimulus onset in milliseconds.

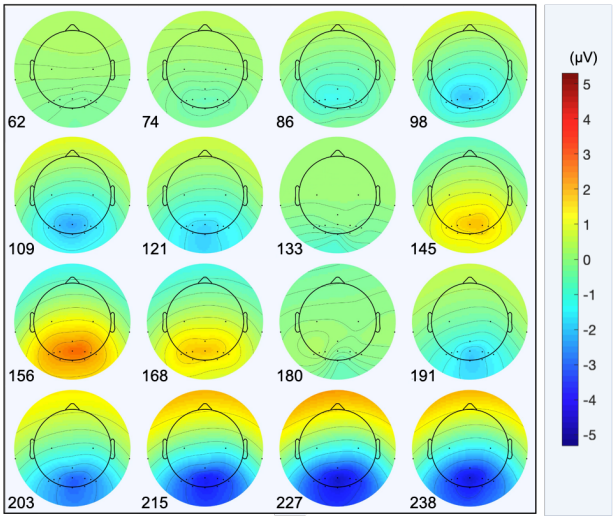

Figure 13. Visual fields difference ERP topographies of the grand average.

However, the C1 component is known to be difficult to observe in the raw ERP data especially in the upper visual field, because it is often combined with P1 component, a

positive going component that arises from both upper and lower visual field stimulation at about the same time, or possibly later (Di Russo et al., 2001). One way of isolating C1 is to subtract the lower visual field data from the upper visual field data, to produce a single negative going peak. Results of such a subtraction are shown in Figure 13, and its topography confirmed a negative going component around 100 ms, that is characteristic of C1.

Mean amplitude ERP

To quantify the amplitude of C1, we averaged the ERP data within a range of ±16 ms around the component's peak in time for each subject. These analyses required identifying the latency where C1 reached its maximum/minimum amplitude (depending on visual field) as well as selecting the electrodes where this peak occurred. We did this by examining the ERP topographies separately for upper and lower visual fields (see Figure 12), and picking the C1 peak location and latency by hand. Mean amplitudes were then compared between conditions using standard statistical methods (t-tests and ANOVAs).

We used two different sets of topographic information to guide peak selection and computation of C1 amplitudes. One used the peaks from the grand average ERPs (Figure 12) to pick a single C1 peak latency and electrode to be used for all subjects. We refer to this as Grand average Peak Selection (GPS). The other used each individual subjects' topographic data to pick their own C1 peak latency and electrode. That is, for each subject we picked the latency and electrodes that showed the strongest response in the topography around the time expected of C1. This will be referred to as

Individualized Peak Selection (IPS), and Table 1 lists the peak latencies and electrodes identified for each subject.

	Peak Latency (ms)				Electrode			
	Pre		Post		Pre		Post	
Subject	**LVF**	**UVF**	**LVF**	**UVF**	**LVF**	**UVF**	**LVF**	**UVF**
Grand Average	102	117	102	117	POz	POz	POz	POz
S01	117	109	117	109	Oz	POz	Oz	PO4
S02	98	117	94	113	PO4	Pz	PO4	Pz
S03	102	117	98	117	PO3	Oz	PO3	Oz
S04	109	129	109	133	PO4	PO3	PO4	PO3
S05	133	133	137	133	POz	PO4	Oz	PO4
S06	98	117	98	117	O1	PO4	O1	PO4
S07	98	117	102	117	O2	Oz	POz	Oz
S08	102	105	98	105	PO3	POz	PO3	Pz
S09	109	121	121	121	Oz	PO8	POz	POz
S10	102	121	102	121	O2	PO3	O2	PO3
S11	125	121	125	121	Oz	POz	Oz	POz
S12	94	121	94	121	POz	PO6	Pz	PO6
S13	98	90	102	94	POz	PO3	POz	PO3
S14	98	121	102	121	Oz	POz	POz	O2

Table 1. List of peak latency and electrode for grand average and individual subjects

Smoothing spline ANOVA (SSANOVA)

Computing mean amplitude involves averaging a range of time points, which might ignore the continuously changing nature of the continuous data. Smoothing spline ANOVA is a method to model, and look for differences in, the smooth functional form of the ERP time course. It is essentially a non-parametric extension of linear mixed effect models. It is beneficial for analyzing data such as ERP, because it pulls out a limited set of functional components (modeled as spline curves) from the continuous data to identify where in the time course differences exists.

The method uses a spline approach, fitting a smooth curve, comprised of multiple cubic functions connected with 'knots', to noisy data. The fits are used to estimate a main effect between conditions and random effects tied to individual subjects. The greater the numbers of knots, the better the model fit, but at an increase of the number of model parameters. Fitting the current dataset was stable with 20 knots or higher, so 20 knots were chosen in the analysis.

We used SSANOVA to test whether adaptation differentially affected response to the vertical and horizontal stimulus. This is in principal, a 2 (visual field) × 2 (orientation) × 2 (pre vs post adaptation) analysis. To reduce the complexity of the analysis, we removed one factor by first computing difference scores between the vertical and horizontal conditions. That is, the input to the analysis was the mean time course (average epochs) from these two stimulation conditions, subtracted from each other for each subject. We tested, for each visual field, whether this difference time course changed as a function of adaptation.

In the analysis, subject was a random effect and adaptation (pre- vs. post-test) was a fixed effect in the model. Separate analyses were run for upper and lower visual field data. Plot of model fits with estimated Bayesian confidence intervals were used to examine differences between conditions, with non-overlapping confidence intervals being interpreted as significant. The execution of the fitting was done by 'bigsplines' package in R (Helwig, 2018; R Core Team, 2019).

Classification analyses

It is additionally possible that effects of adaptation will mainly be visible as changes in the spatial pattern of activity across the set of electrodes that are difficult to observe in individual ERP components at single electrodes. The ERP waveform analyses and the SSANOVAs were conducted separately for each electrode, and so cannot test for this possibility. To test if the spatial pattern of activity changed due to adaptation, we used a standard classification analysis. Support vector machines (SVM) were used to classify data across electrodes as arising from vertical vs horizontal stimuli. If adaptation had a selective effect on one orientation, then classification performance should improve.

The classification analysis took as input the topographies (see Figure 12) of EEG signal across electrodes at one timepoint. A support vector machine was then trained on the voltage at that time point in multiple epochs from each condition to predict the stimulus condition (vertical or horizontal) from the EEG topography. This analysis was repeated for all timepoints in the ERP trace.

To reduce noise in the topographies, we trained the SVM on average epochs, which were data averaged across 10 randomly selected epochs (without replacement). Data were also smoothed by taking a moving average of 3 timepoints. These choices for noise reduction were not critical for obtaining the observed pattern of results, but did increase their reliability. To make sure results were not dependent on the particular sampling used for the epoch averaging, SVM training was repeated 10 times, with the dataset sampled and averaged differently every time.

We fit the SVM classifier using a standard 10-fold cross-validation procedure, implemented by MATLAB's 'kfoldLoss' function. As a measure of classification performance, we used the cross-validation loss, which indicates out-of-fold misclassification rate. We converted this to percent correct classification and averaged across our 10 repetitions of data sampling, epoch averaging, and model training.

2.3 Results

2.3.1 ERP Waveform

Figure 14, plots the grand mean ERPs, averaged across subjects from the three electrodes Pz, POz, and Oz. Data from trials with vertical and horizontal orientations are shown in red and blue, respectively, and data from trials in the upper visual field are indicated with dotted lines, and from the lower visual field with solid lines. These same plotting conventions will be used in all subsequent figures.

The data show the C1 component, visible in the peaks in the ERP time courses around 100 ms; the polarity of this peak flips when the stimulus was presented in the upper vs lower visual fields, though perhaps unexpectedly it is relatively delayed for horizontal stimulation. This polarity flip is characteristic of C1, and is expected due to the retinotopic representation and the folded shape at calcarine fissure in V1, where the C1 component is assumed to be generated (Clark, Fan, & Hillyard, 1995).

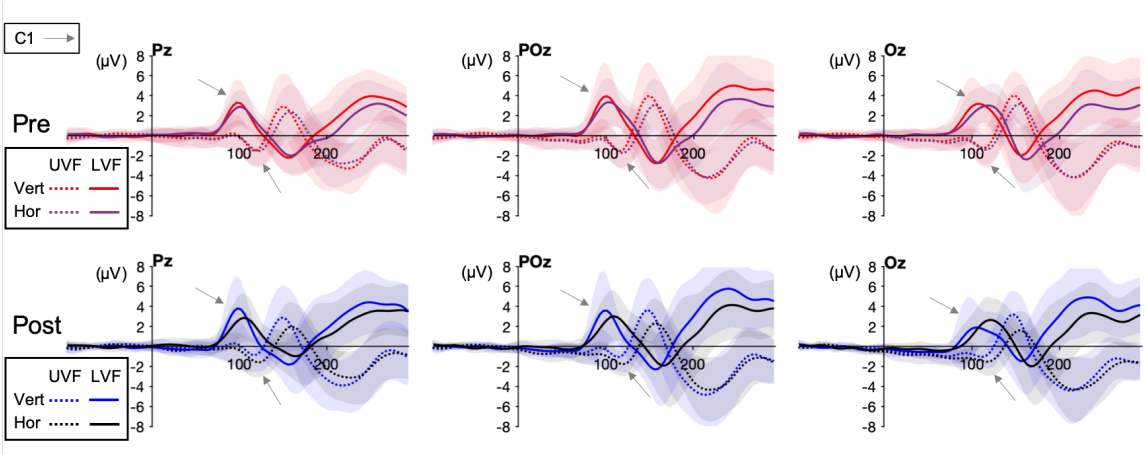

Figure 14. Grand average ERP waveforms from three electrodes, Pz, POz, and Oz. C1 components are indicated with the arrows. Shaded areas indicate s.e.m.

Our hypothesis was that adaptation/deprivation would increase response in early visual cortex. We expected this to be visible in the ERP data as larger responses for the deprived orientation, which was vertical. Since higher stimulus contrast induces earlier phase of VEP (Burr & Morrone, 1987), we also expected vertical responses to arise early in time. We will call the size of the responses its amplitude, and the timing of the response its latency.

2.3.2 Mean Amplitude

Figure 14 shows that the amplitude of the C1 peak (near 100 ms) was slightly greater for vertical than for horizontal stimuli. Even in the pre-adaptation test, there was a slight difference between vertical and horizontal orientation curves in this first peak, especially in the lower visual field.

Adaptation may have increased the difference between C1 responses to vertical and horizontal. While it is not obvious that the *absolute* amplitude of the vertical response is increased in the post-test compared to the pretest, the *difference* between the vertical

and horizontal responses appears larger in the post-test than in the pre-test. To test the statistical significance of these trends, we calculated C1 amplitudes for each condition, by averaging 32 ms centered around the timepoint of the peak.

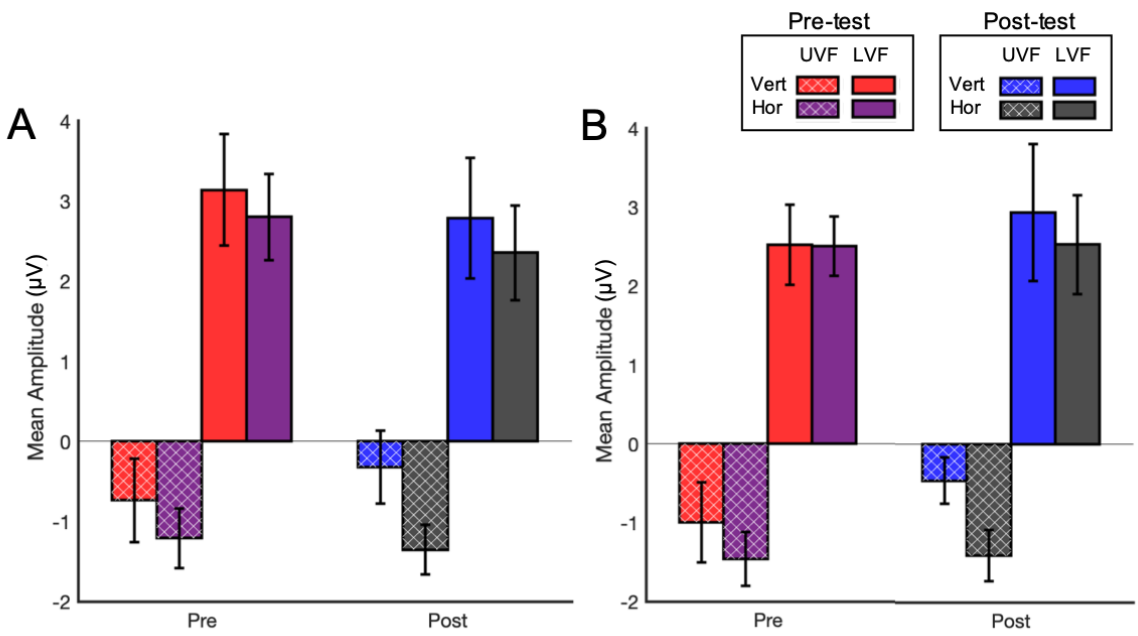

Figure 15. ERP mean amplitudes. (A) Mean around the peak of grand average ERP (GPS). (B) Mean around individual subjects' peak latency and electrodes (IPS). Error bars indicate ±1 s.e.m.

Figure 15 plots C1 mean amplitudes. Computing a mean amplitude requires picking a specific time and electrode over which to average (See Methods). The analysis shown in the left panel used the grand average ERP to define the electrode and timepoint of the peak of the C1 visible in the ERP topography (e.g. Figure 12; GPS). The right panel shows results when the peak timepoints and electrodes were picked separately for each subject, by examining their own average ERP topographies (IPS). The most consistent effect shown here is that the difference between vertical and horizontal was larger in the post-test than in the pre-test.

To test the reliability of these effects we ran separate repeated-measures ANOVAs for upper and lower visual fields with session (Pre- vs. Post-test) and stimulus orientations (Vertical vs. Horizontal) as within-subject factors. The main effect of stimulus orientation was significant only in the upper visual field ($F(1,13) = 9.171$, $p=.010$ with GPS; $F(1,13)=11.49$, $p=.005$ with IPS). The main effect of adaptation was not significant in either of the cases ($F(1,13)=.324$, $p=.579$ with GPS, and $F(1,13)=.567$, $p=.465$ with IPS). There was no significant interaction between session and orientation, either using GPS or IPS, indicating that the difference between vertical and horizontal responses did not significantly change after adaptation.

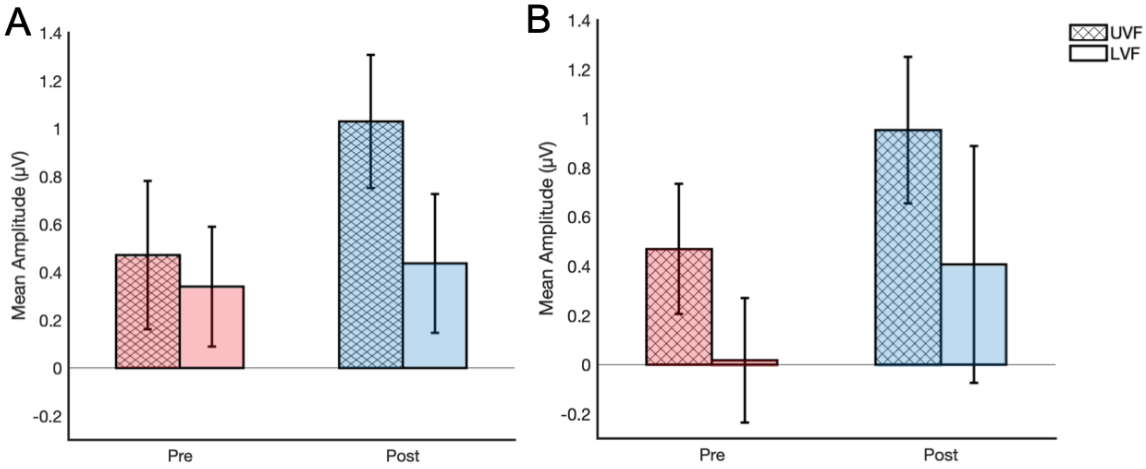

Figure 16. Difference of ERP amplitudes to vertical and horizontal stimulation. (A) Mean around the peak of grand average ERP. (B) Mean around individual subjects' peak latency and electrodes. Error bars indicate ±1 s.e.m.

Figure 16 plots the difference between vertical and horizontal amplitudes. While there was a trend for larger differences following adaptation, this did not reach statistical significance (Main effect of Session: $F(1,13)=3.10$, $p=.102$ with GPS and $F(1,13)=2.47$, $p=.140$ with IPS; Main effect of Visual field: $F(1,13)=1.39$, $p=.260$ with GPS and

F(1,13)=1.80, p=.202 with IPS). There was no significant interaction between the factors (F(1,13)=1.61, p=.226 with GPS and F(1,13)=.05, p=.834 with IPS).

2.3.3 Peak Latency

C1 latencies for vertical and horizontal stimuli also appeared to differ slightly, with the vertical response peaking slightly before the horizontal for the first peak in the lower visual field. This difference in peak latency between orientations appears larger in the post-test.

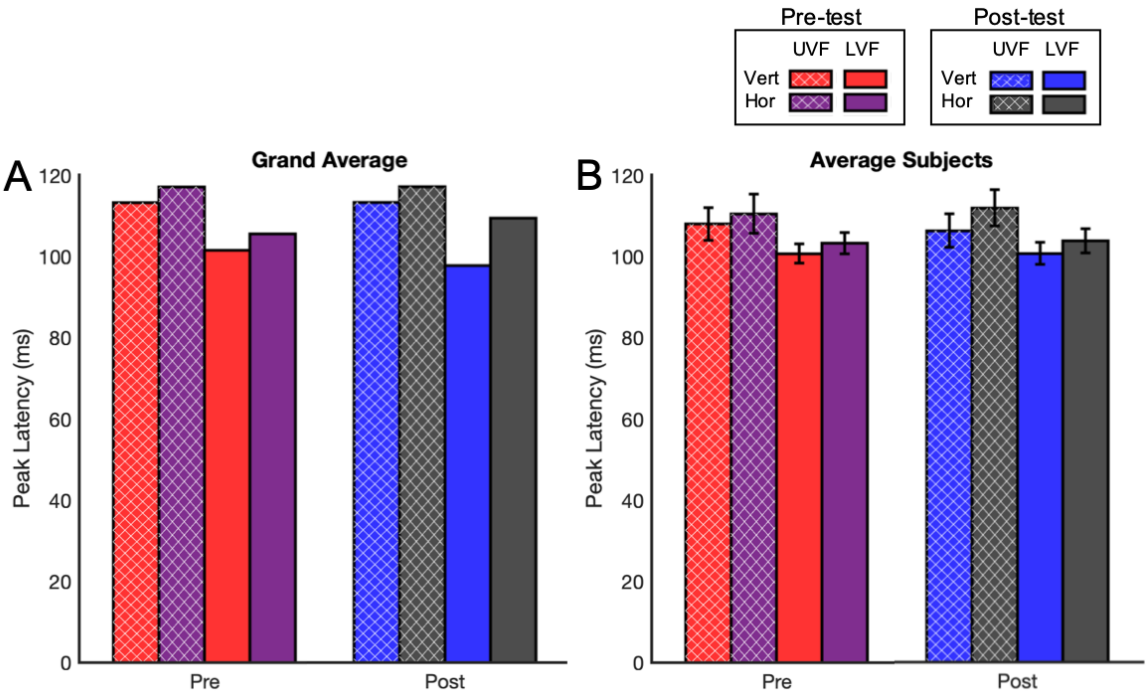

Figure 17. ERP peak latencies (A) Grand average ERP peak latency, picked from grand average topographies. (B) Average of individual subjects' ERP peak latencies picked from each individual's topographies. Error bars indicate ±1 s.e.m.

Figure 17 summarizes the peak C1 latencies, with separate bars for vertical and horizontal, upper and lower visual field, and pre- and post-tests. The latencies of Figure 17A are picked from the grand mean ERPs topography, and those of Figure 17B are

picked from each individual subjects' topographies and averaged across subjects. The figure shows an overall trend for lower latencies for vertical than horizontal. This trend is slightly larger in the post-test than in the pre-test in some cases.

We tested the statistical significance of these differences with a $2 \times 2 \times 2$ repeated measures ANOVA with orientation, visual field, and pre-post as factors. This analysis found significant effect of orientation ($F(1,13)=13.31$, $p=.003$). However, the effect of Session and Visual Field did not reach significance (Session: $F(1,13)=.01$, $p=.939$; Visual Field: $F(1,13)=3.06$, $p=.104$). Specifically, our hypothesis of stronger response to vertical following adaptation predicts an interaction between session and orientation, where vertical latencies may have declined but horizontal latencies may have been unaffected. This interaction approached, but did not reach significance ($F(1,13)=3.344$, $p=.090$).

2.3.4 SSANOVA

To test for possible effects of adaptation across the entire time course, we used an analysis technique called Smooth-Spline ANOVA, which contains an explicit model of the EEG signal over time (See Methods, above). The method uses these models to test for systematic differences in the time course between conditions. Two-way SSANOVAs are easiest to interpret, and we report these below; we reduced the dimensionality of the problem by analyzing upper and lower visual field responses separately, and by examining difference scores between responses to vertical and horizontal stimulation. The SSANOVA analysis also faced the challenge of electrode selection, like the ERP analyses did, and we used the same two methods of electrode selection here: GPS and IPS.

Our hypothesis was that adaptation would increase the difference between vertical and horizontal responses, which would be visible as a larger difference score. We were particularly interested in differences arising relatively early in time, as these could arise from C1.

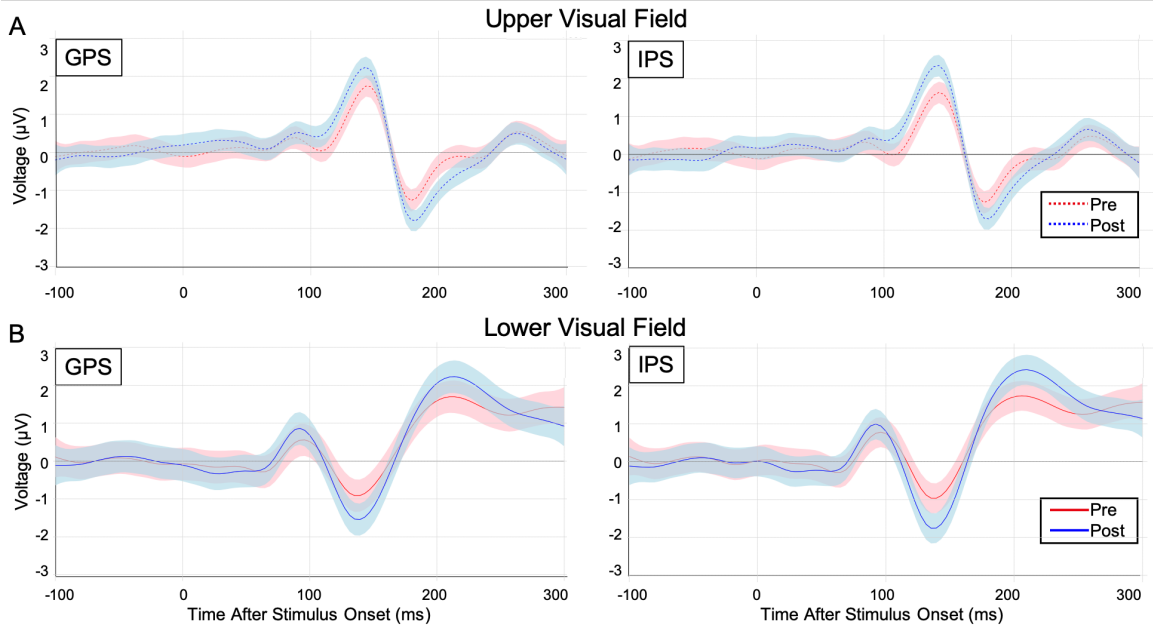

Figure 18. Pre- vs. Post-test SSANOVA. [Vertical – Horizontal] ERP difference fitted with SSANOVA, plotted with 95% Bayesian confidence interval (shaded) for Pre-test (red) and post-test (blue).

Figure 18 plots the results of the SSANOVA, with model-based estimated difference time courses surrounded by 95% Bayesian confidence intervals. Plots are shown for pre- and post-tests, and upper and lower visual fields. We will interpret non-overlapping confidence intervals between pre- and post-test to indicate the change in orientation difference after adaptation.

The fitted curves show an initial peak in the difference score at around at around 90 ms in the lower visual field, which roughly corresponds to the C1 response from the ERP analysis. Results from both visual fields show a larger peak at around 140 ms, with the peak going positive in the LVF and negative in the UVF. These peaks are also visible in the ERP and may correspond to a secondary response following C1 (more on this in Interpretation, below).

The most significant differences between the pre- and post-test confidence intervals was found in the upper visual field at around 110-140ms using IPS (Figure 18). Similar, but slightly less significant differences were found at the same time in the lower visual field, though the peaks were negative going. Some additional hints of effects of adaptation were found at a third peak at 180-200 ms, which was again of reversed sign from the previous peak in both visual fields.

Because adaptation weakens over time, it is possible that the change in orientation difference would appear only in some part of the post-test data. To explore this possibility, we conducted extra SSANOVAs that examined only the 1st half or 2nd half of the post-test data (Figure 19-20).

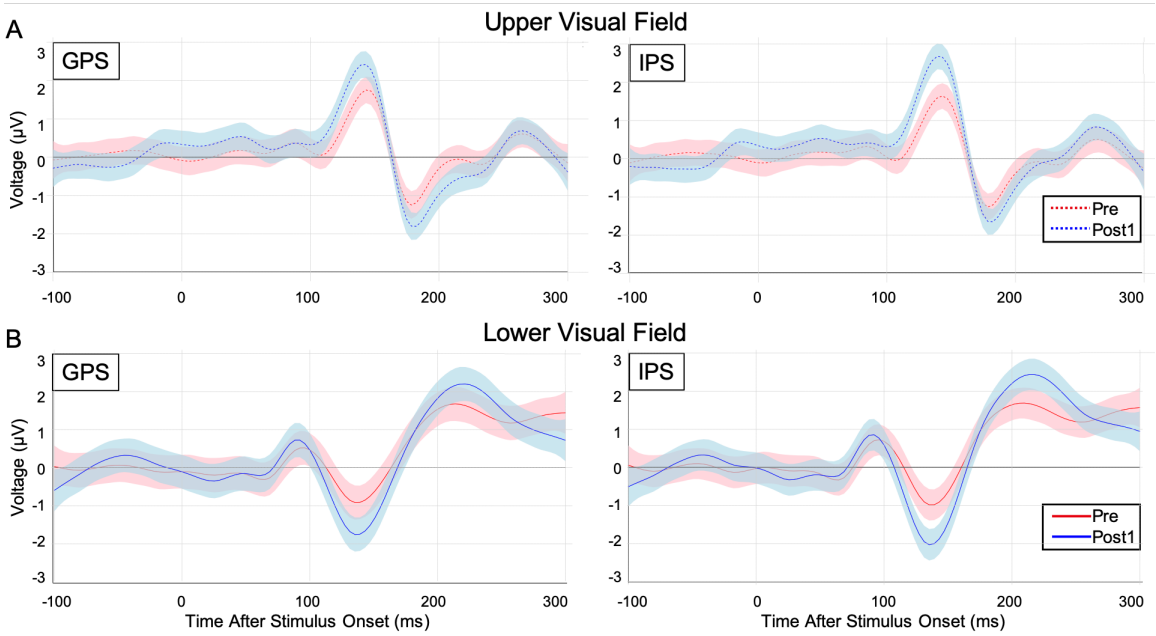

Figure 19. Pre- vs. 1st half of Post-test SSANOVA. [Vertical – Horizontal] ERP difference fitted with SSANOVA, plotted with 95% Bayesian confidence interval (shaded) for Pre-test (red) and post-test (blue).

In general, the same pattern of results obtained, but effects of adaptation were more significant when the pre-test was compared with the 1st half of post-test. This revealed more significant effects at the peak around 140 msec in all analyses (Figure 19). As expected, effects of adaptation were reduced when examining data from the second half of the post-test (Figure 20).

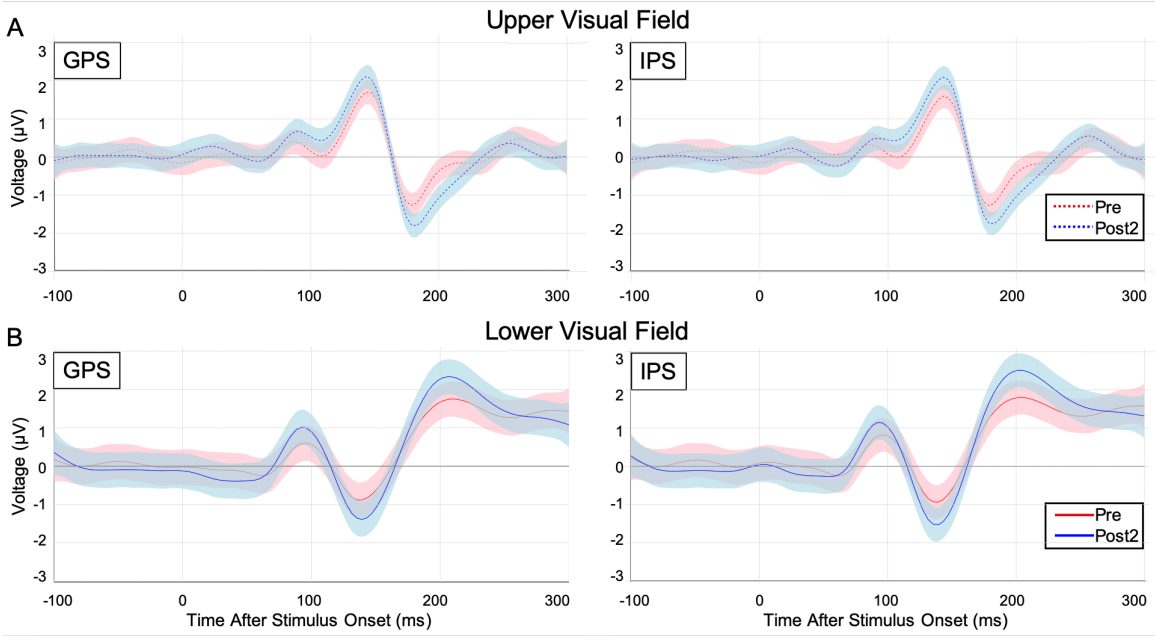

Figure 20. Pre- vs. 2nd half of Post-test SSANOVA. [Vertical – Horizontal] ERP difference fitted with SSANOVA, plotted with 95% Bayesian confidence interval (shaded) for Pre-test (red) and post-test (blue).

2.3.5 Classification Analyses

To test the possibility that the adaptation effect is more clearly shown as changes in the spatial pattern of activities across multiple electrodes, we ran a classification analysis on the data. The goal of the classifier was to categorize a given pattern of ERP response based upon the pattern of activity that produced it. We hypothesized that if adaptation differentially affected responses to vertical and horizontal stimulation (i.e. increasing responses to vertical relative to horizontal), then the classifier should be better able to distinguish between them following adaptation. We used linear support vector machines to perform the classification (see Methods).

The accuracy of classifying vertical and horizontal data is plotted in Figure 21. Lines show classification accuracy at each timepoint, averaged across the subjects, error

ribbons are the standard error of the mean accuracy, and significant results of paired t-tests between accuracies from pre- and post-test data are marked as yellow dots.

Decoding accuracy was generally higher in the post-adaptation data, indicating that the classifier was able to differentiate vertical and horizontal orientations better after the 4-hour adaptation. The accuracies started to rise at around 70 ms and reached a first local maximum at around 90 ms after stimulus onset both in the pre- and post-tests, roughly corresponding to the latency range of C1. A Wilcoxon Signed-Ranks Test indicated that there was a significant difference between the maximum accuracy at this early peak in the pre-test (Median = 54.89%) and the post-test (Median = 62.56%), in the upper visual field ($Z=2.92$, $p=.002$, $r=.78$). This trend was consistent in the lower visual field ($Z=2.23$, $p=.025$, $r=.60$), indicating a significant difference between the classification accuracies of the pre-test (Median = 57.83%) and the post-test (Median = 71.45%).

Later peaks in decoding accuracy also showed effects of adaptation. These fall around the times that the SSANOVA analyses also found significant changes in the difference in responses vertical and horizontal.

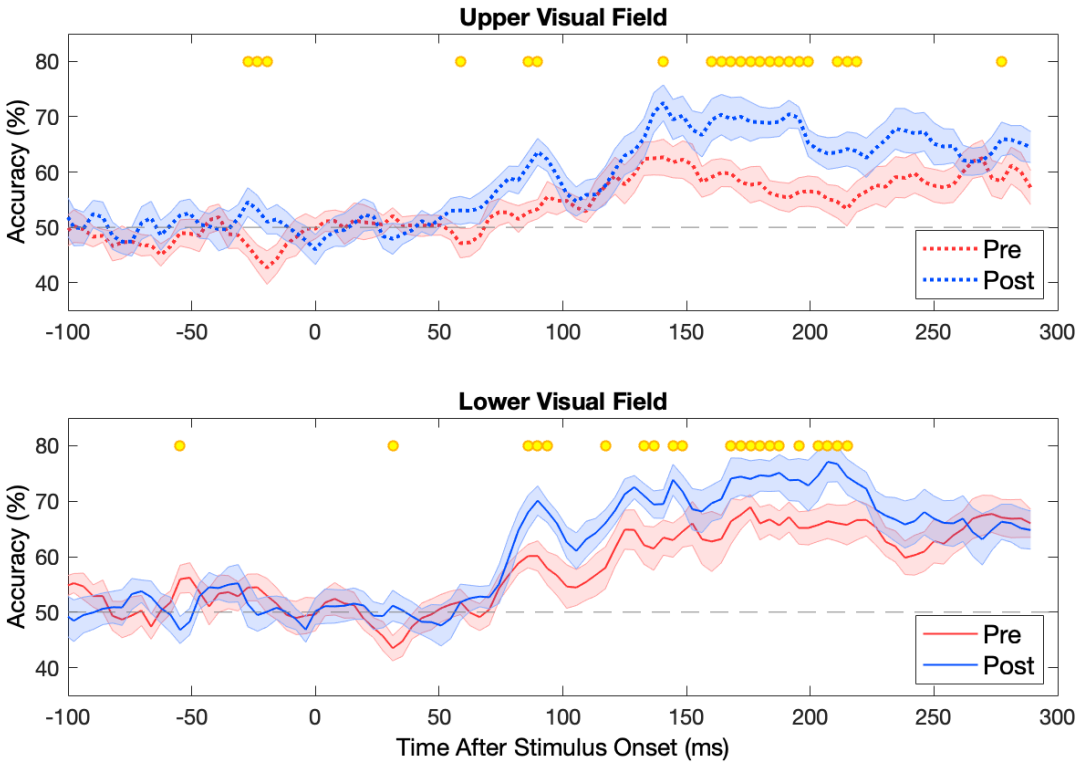

Figure 21. SVM classification results. The accuracies classifying vertical and horizontal orientations are plotted. Shaded areas indicate s.e.m. Chance level is at 50% (dashed line). Yellow dots indicate the timepoints when Wilcoxon Signed-Ranks Tests were significant ($p < .05$).

2.3.6 Interpretation

The ERP results show several peaks in the time courses. Encouragingly, the peaks we observed are generally consistent with past results. Di Russo and colleagues (2001) found a similar pattern (Figure 22) in one of the most thorough investigations of early visual potentials. Their waveforms from POz look very similar to ours, showing an initial C1 peak that flips sign for upper vs lower visual field stimulation, and a secondary peak later in the time course, that is also opposite sign for upper and lower visual fields.

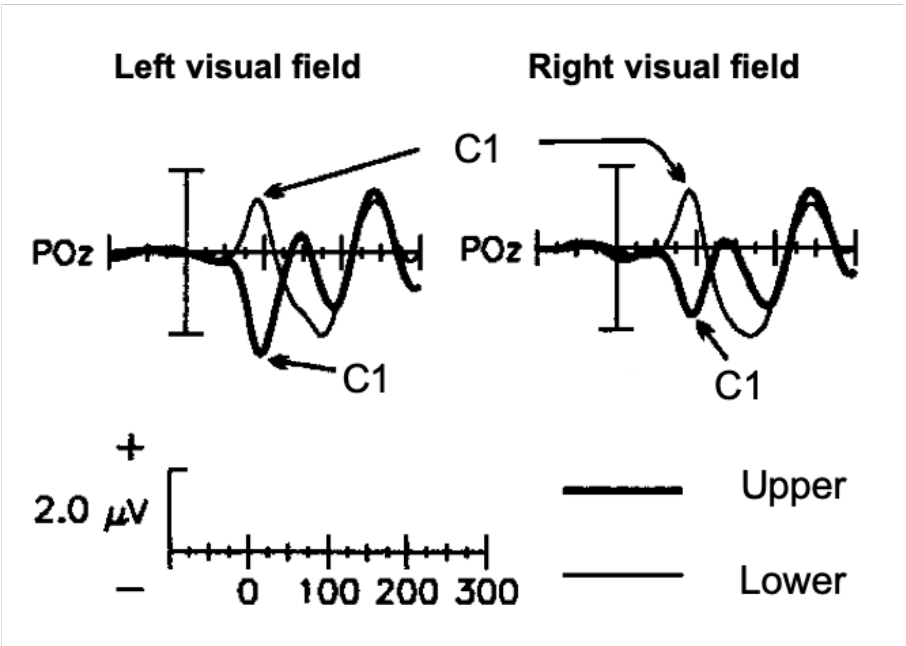

Figure 22. ERP waveforms showing C1 components in previous work (Di Russo et al., 2001). Grand average ERP waveforms from measured for 80% contrast circular checkerboards in the four quadrants. Plots from POz electrodes are shown here. The polarity is flipped from the original plot, so that positive voltage is upward, to make easier comparison to the plots in the current paper. Adapted from Di Russo et al. (2001).

Figure 23 summarizes the results from three analyses, ERP, SSANOVA, and classification, in a way designed to facilitate comparison between the different results, with C1 and the secondary peak highlighted. Shaded areas indicate the timing of the C1 peak in upper and lower visual fields, along with the timing of the following peak in the ERP.

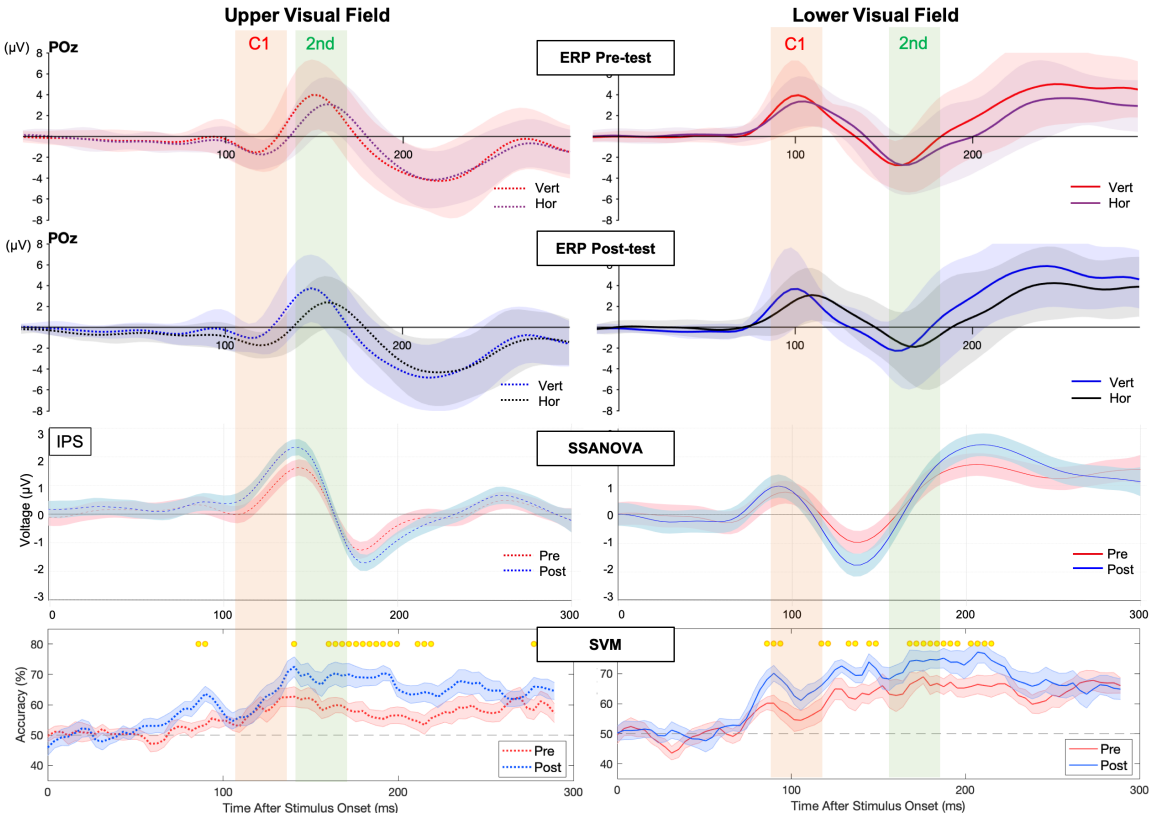

Figure 23. Comparison across analyses. Representative results from ERP wave, SSANOVA, and SVM, with the stimulus onset time are aligned at 0-300ms. Note that the electrodes included for analyses in these figures are different.

Our primary hypothesis was that C1 would increase in amplitude and possibly decrease in latency for vertical, relative to horizontal, following adaptation. We observed a trend for this pattern in the ERP waveform from the LVF stimulation (Figure 23, right panel), but the statistics with mean amplitude and latency did not show a significant effect. In addition, the Bayesian confidence intervals of the SSANOVA plot around the time of C1 overlapped for LVF stimulation again indicating there was no significant change in response to vertical relative to horizontal after adaptation. For UVF stimulation, the confidence intervals did not overlap, suggestive an effect of adaptation on C1, though the direction of this was opposite of that expected. The classification analysis showed

some time points before and after C1 where accuracy was significantly higher following adaptation, which also suggests an effect of adaptation on C1.

Collectively, then, our results provide mixed evidence on whether C1 is affected by adaptation, with perhaps more support for the hypothesis than against it. It seems possible that there was an effect on C1, but that we mainly see significance in the classification analysis because that method simply has the most statistical power, gained by pooling across all electrodes.

The secondary peak also shows evidence of being affected by adaptation. In the ERP, for stimulation in both visual fields, the main visible change was in latency of the peak, with response to vertical stimulation occurring earlier in time, relative to horizontal stimulation, following adaptation.

The SSANOVA results show a particularly interesting pattern surrounding the second peak. On both sides of the peak, there are bigger differences between vertical and horizontal response after adaptation. These differences are in opposite directions on the two sides of the peak. This is precisely the pattern one would expect from the change in latency of vertical relative to horizontal visible in the ERP, which led to greater response to vertical before the peak, and greater response of horizontal after the peak. This pattern may also apply in the upper visual field to the SSANOVA results surrounding the C1 peak. The classification analysis again showed a broadly similar pattern, with significantly better decoding following adaptation on either side of the secondary peak. Overall then, there is fairly substantial evidence that the secondary peak is affected by adaptation.

Why was C1 so small in the UVF? Di Russo et al. (2001), suggested that the negative going C1 could be canceled by a positive peak, P1, with similar latency range that arises with a different cortical generator, probably extrastriate cortex. This could be the case in our data as well. Under the assumption that both C1 and P1 are generated from both visual fields, but that only C1 flips signs, we can isolate C1 by subtracting the UVF from the LVF waveform. Similarly, we can isolate P1 by adding the two waveforms.

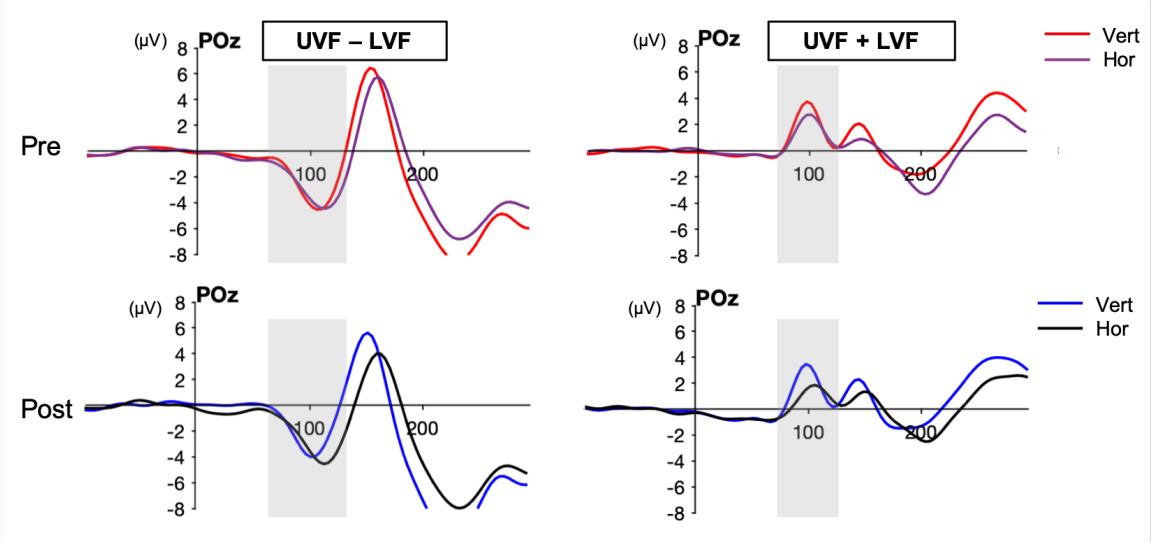

Figure 24. Visual fields difference (left) and summation (right) waves from POz electrode of pre- (top) and post-test (bottom) ERP data.

Results of this subtractions and addition are shown in Figure 24, which plots sum and difference waves of the ERP. There are two observations that may be relevant to understand the mixed results of the above analyses. The difference wave shows a latency shift of the vertical response in the post-test, along with surprisingly, a small decrease in amplitude. The summation wave shows decrease in amplitude of horizontal condition after adaptation, which leads to the greater difference between vertical and

horizontal. The combination of these two may explain the changes in discriminability of orientations following adaptation found in SSANOVA and classification analyses.

While suggestive, we have not pursued extensive analyses of the sums and difference waves in part because it is known that upper and lower visual field stimulation will activate quite different parts of early visual cortex, making combining responses in this way potentially problematic. Full cortical-based modeling of multiple underlying neural generators of the ERP would solve this problem, and is an interesting direction for future research.

Ch 3. General Discussion

This study tested the hypothesis that long-term adaptation can change responses in early visual cortex. Overall, our results support the hypothesis, though many predicted effects did not reach significance. Specifically, we found the mean amplitude of the C1 component for the deprived orientation, vertical, did not significantly increase after adaptation.

However, we found a trend for the mean amplitude *differences* between vertical and horizontal conditions to be greater in the post-test, as well as a trend for the latency difference between the two conditions to increase. This suggests that adaptation may have affected both orientations. Accordingly, examining the vertical and horizontal difference, which shows relative change, or examining pattern discriminability for the two orientations, may better reveal the adaptation effect.

Several analyses did find that adaptation affected the relative strength of vertical and horizontal responses. The SSANOVA results showed a significant gap of orientation difference score between pre- and post-test at early timepoints. We also found that the performance of SVM classifier decoding deprived vs the other orientation improved after adaptation. In sum, it seems likely that long-term adaptation did change early visual cortical responses, but these effects may be smaller than expected, leaving our basic ERP analyses not significant. The more sensitive SSANOVA and classification analyses did show effects of adaptation on early visual responses.

3.1 Future Work: Additional Analyses of Current Data

A number of unresolved issues arise from the current data, and suggest analyses that could be addressed in future work. Most importantly, we have not examined the spatial aspects of the classification results. It would be interesting to determine the pattern of changes in ERP response across the cortical topography that leads to better classification following adaptation. This could be examined by the weights on the electrodes that reflect which electrodes contributed more to deciding the classifying hyperplane at each timepoint. Haufe and colleagues (2014) introduced a spatial weight projection method where classifier weights are transformed back to activation patterns. By multiplying the classifier weights with the covariance in the data, resulting reconstructed pattern can be projected on the scalp map (Grootswagers, Wardle & Carlson, 2017). Applying this method will show the locations of more informative electrodes at different timepoints in our data.

Relatedly, while we closely examined the spatial topography for the C1 component, we have not examined the topography closely for the secondary peak. Eyeballing the voltage topography shows a positive focus around 150ms at posterior midline for UVF stimulus, and bilateral negative foci around 160ms for UVF stimulus (Figure 12), suggesting that these sources may be quite different.

Another related direction would be to examine differences in response around even later components of the ERP. The average time courses show a third peak after 200ms. The topography of UVF stimulus shows negative foci around 200ms (Figure 14), which is about the same location seen in the LVF topography at the latency range of the second

peak (Figure 12). It is difficult to interpret whether showing similar topographies reflect that they originate from the same brain structure because EEG is measured at the scalp and more components would be compounded especially in the later time course of ERP.

One way to distinguish ERP components using topography is to conduct a source analysis to try to identify the location of neural generators of the different components. These analyses could in theory be run on our current data, though the small number of electrodes we recorded from make them challenging. In addition, source analyses benefit greatly from including individual subject MRI scans (Di Russo et al., 2001).

3.2 Procedural Caveats

A number of procedural concerns also may affect the interpretation of our results. Most importantly, we cannot be sure whether the changes in EEG measured at the end of 4-hour adaptation are solely due to long-term adaptation, because the current experiment did not test shorter adaptation durations. It is possible we would have observed very similar results following these shorter durations. This in turn would suggest that the effects we observed were due to short-term adaptation that was simply maintained by the ongoing presence of the adapting stimulus over the 4-hour period.

A second concern is the number of subjects that were excluded. Out of 28 subjects who completed both pre- and post-test sessions, we report analyses with only 14 of them who survived our data quality checks. Early ERPs can vary across individuals due to cortical geometric variability in V1 (Foxe & Simpson, 2002; Proverbio, Zotto, & Zani, 2007). Including more subjects and considering individual differences could increase the

statistical power of our study. New procedures should be developed to allow for a greater percentage of subjects to provide data of acceptable quality.

The current experiment did not entail behavioral measures of adaptation. Common behavioral methods to measure orientation-selective contrast adaptation such as contrast matching or TAE were difficult to incorporate into our ERP paradigm. Measuring TAE requires displaying test patterns at off orientations, which would have reduced our available data collection time for horizontal and vertical. Contrast matching and contrast detection methods did not suit our purposes either, because varying the contrast of test stimuli will add extra variability to our measurements of early components of ERP.

3.3 Future Work: Follow-up Study

It would be relatively straightforward to design a follow-up study to address many of these procedural concerns. Changes could include:

1. Optimize stimulus to see better C1 polarity inversion. It has been known that the point of the polarity inversion of C1 is not exactly at the horizontal meridian of the visual field. It is more commonly found at about polar angles of 10-20° below the horizontal meridian (Aine, Supek, & George, 1995; Clark, Fan, & Hillyard., 1995; Di Russo et al., 2001). Even though our stimuli locations were at vertical meridian, the nearest distance between the gratings and center fixation point was only 0.5° which might not be a perfect location to see the polarity flip of C1. Additionally, separating left and right visual field stimulation may enhance the EEG signal considering the retinotopic representation of early visual field which is separate in the left and right hemispheres.

2. A potential way to separate C1 and P1 components other than source localization is to increase the contrast of test stimulus. Whereas C1 response increases as a function of stimulus contrast of 11% and higher, P1 increases within contrast 4-16%, then saturates with the higher contrast (Foxe et al., 2008). These results suggest that the two components depend differentially upon parvocellular (P) and magnocellular (M) input, with C1 being dominated by P and P1 being dominated by M. The current study used a contrast of 15%. Increasing that contrast level may increase the relative strength of the contribution from C1 in our early peak.

3. Measure effects also after shorter durations (e.g. 10, 30, or 60 minutes) of deprivation, to distinguish between short-term and long-term adaptation. Different mechanisms may control visual adaptation over different time scales, and differences in results between shorter and longer protocols could isolate effects due to long-term mechanisms. It would be best to run separate sessions for short-term and long-term adaptation because testing after a shorter duration of adaptation inevitably induces some amount of de-adaptation. Having data at more adapting durations, could also allow us to fit build-up functions to the time course of adaptation.

4. Measure behavioral effects of adaptation and correlate these with EEG results. As stated above, it is challenging to measure ERP and behavioral effects of adaptation using the same stimulus. However, we can measure the effect of adaptation using a behavioral method that does not show the deprived orientation such as TAE. Though indirect, it would enable comparing ERP results and behavioral measures of adaptation.

5. Future work could revisit this study while also acquiring individual MRI scans and greater numbers of EEG electrodes to allow for better source localization. Another approach is to partition the EEG responses into sources from known visual areas, identified using retinotopic mapping, either from atlases or from fMRI individual subjects (Di Russo et al., 2001; Norcia et al., 2015)

6. In might be preferable to enhance contrast at the adapting orientation rather than deprive it. Deprivation could, in theory, be more vulnerable to de-adaptation during testing that enhancement, since viewing any vertical information at all could lead to de-adaptation.

3.4 Alternative Interpretation

It is possible that the changes we observed in early visually evoked potentials could also reflect attentional effects. Vertical stimuli may grab attention more than horizontal ones post-adaptation because the vertical stimulus was deprived for a long duration. Whether C1 can be altered by attention is debatable, with many studies finding that it is not affected by attention (Di Russo, Martinez & Hillyard, 2003; Gomez-Gonzales et al., 1994; Hillyard, Vogel & Luck, 1998), but others finding that attention can affect it (Kelly, Gomez-Ramirez, & Foxe, 1998; Zani & Proverbio, 1997).

An interesting future direction could distinguish between attentional effects and more bottom-up changes. It would be possible to repeat this study but with attention either focused on the test stimuli or directed elsewhere (e.g. a demanding fixation task).

Should our results replicate even when test stimuli are unattended, it would support the feedforward gain change hypothesis.

3.5 Conclusions

Long term adaptation to deprivation of an orientation can alter the relative strength of C1 and other early components. This suggests that it may increase the gain of feedforward signals in early visual cortex. This interpretation matches our original hypothesis, as well as the prior short-term adaptation literature that reported gain changes in the early visual cortex (Bach, Greenlee & Bühler, 1988; Heinrich & Bach, 2001; Mecacci & Spinelli, 1976; Rebaï & Bonnet, 1989).

Bibliography

Abbonizio, G., Langley, K., & Clifford, C. W. (2002). Contrast adaptation may enhance contrast discrimination. *Spatial Vision, 16,* 45–58.

Aine, C. J., Supek, S., & George, J. S. (1995). Temporal dynamics of visual-evoked neuromagnetic sources: Effects of stimulus parameters and selective attention. *International Journal of Neuroscience*, *80*(1–4), 79–104.

Albrecht, D. G., Farrar, S. B., & Hamilton, D. B. (1984). Spatial contrast adaptation characteristics of neurones recorded in the cat's visual cortex. *The Journal of Physiology*, *347*(1984), 713–739.

Bach, M., Greenlee, M. W., & Bühler, B. (1988). Contrast adaptation can increase visually evoked potential amplitude. *Clinical Vision Science*, *3*(3), 185–194.

Bao, M., & Engel, S. (2012). Distinct mechanism for long-term contrast adaptation. *Proceedings of the National Academy of Sciences of the United States of America*, *109*(15), 5898–5093.

Bao, M., & Engel, S. A. (2019). Augmented Reality as a Tool for Studying Visual Plasticity: 2009 to 2018. *Current Directions in Psychological Science*. https://doi.org/10.1177/0963721419862290.

Bao, M., Fast, E., Mesik, J., & Engel, S. (2013). Distinct mechanisms control contrast adaptation over different timescales. *Journal of Vision*, *13*(10), 1–11.

Barlow, H. B. (1990). A theory about the functional role and synaptic mechanism of visual after-effects. *Vision: Coding and Efficiency*, 363–375.

Bi, T., Cai, P., Zhou, T., and Fang, F. (2009). The effect of crowding on orientation-selective adaptation in human early visual cortex. *Journal of Vision*, *9*(11), 13, 1–10.

Blakemore, C., & Campbell, F. W. (1969). On the existence of neurones in the human visual system selectively sensitive to the orientation and size of retinal images. *The Journal of Physiology*, *203*(1), 237–260.

Boynton, G. M., & Finney, E. M. (2003). Orientation-specific adaptation in human visual cortex. *Journal of Neuroscience*, *23*(25), 8781–8787.

Brainard, D. H. (1997). The psychophysics toolbox. *Spatial Vision, 10*, 433–436.

Burr, D. C., & Morrone, M. C. (1987). Inhibitory interactions in the human vision system revealed in pattern-evoked potentials. *The Journal of Physiology*, *389*(1), 1–21.

Butler, S. R., Georgiou, G. A., Glass, A., Hancox, R. J., Hopper, J. M., & Smith, K. R. H. (1987). Cortical generators of the CI component of the pattern-onset visual evoked potential. *Electroencephalography and Clinical Neurophysiology/ Evoked Potentials*, *68*(4), 256–267.

Campbell, F. W., & Maffei, L. (1970). Electrophysiological Evidence for the Existence of Orientation and Size Detectors in the Human Visual System. *Journal of Physiology*, *207*, 635–652.

Carandini, M., & Ferster, D. (1997). A Tonic Hyperpolarization Underlying Contrast Adaptation in Cat Visual Cortex. *Science*, *276*(5314), 949–952.

Clark, V. P., Fan, S., & Hillyard, S. A. (1995). Identification of early visual evoked potential generators by retinotopic and topographic analyses. *Human Brain Mapping*, *2*(3), 170–187.

Clifford, C. W. G., Webster, M. A., Stanley, G. B., Stocker, A. A., Kohn, A., Sharpee, T. O., & Schwartz, O. (2007). Visual adaptation: neural, psychological and computational aspects. *Vision Research*, *47*(25), 3125–3131.

Delorme, A., & Makeig, S. (2004). EEGLAB: An open source toolbox for analysis of single-trial EEG dynamics including independent component analysis. *Journal of Neuroscience Methods*, *134*(1), 9–21.

Descalzo, V. F., Nowak, L. G., Brumberg, J. C., McCormick, D. A., & Sanchez-Vives, M. V. (2005). Slow adaptation in fast-spiking neurons of visual cortex. *Journal of Neurophysiology*, *93*(2), 1111–1118.

Di Russo, F., Martínez, A., Sereno, M. I., Pitzalis, S., & Hillyard, S. A. (2001). Cortical sources of the early components of the visual evoked potential. *Human Brain Mapping*, *15*, 95–111.

Di Russo, F., Martinez, A., & Hillyard, S. A. (2003). Source analysis of event-related cortical activity during visuo-spatial attention. *Cerebral Cortex*, *13*(5), 486–499.

Dong, X., Engel, S. A., & Bao, M. (2014). The time course of contrast adaptation measured with a new method: Detection of ramped contrast. *Perception*, *43*(5), 427–437.

Dragoi, V., Sharma, J., & Sur, M. (2000). Adaptation-Induced Plasticity of Orientation Tuning in Adult Visual Cortex. *Neuron*, *28*(1), 287–298.

Drew, P. J., & Abbott, L. F. (2006). Models and properties of power-law adaptation in neural systems. *Journal of Neurophysiology*, *96*(2), 826–833.

Duong, T., & Freeman, R. D. (2007). Spatial frequency-specific contrast adaptation originates in the primary visual cortex. *Journal of Neurophysiology*, *98*(1), 187–195.

Fahle, M. (2005). Perceptual learning: Specificity versus generalization. *Current Opinion in Neurobiology*, *15*, 154–160.

Fang, F., Murray, S. O., Kersten, D., & He, S. (2005). Orientation-tuned FMRI adaptation in human visual cortex. *Journal of Neurophysiology*, *94*(6), 4188–4195.

Fine, I., & Jacobs, R. A. (2002). Comparing perceptual learning tasks: A review. *Journal of Vision*, *2*, 190–203.

Fiorentini, A., Pirchio, M., & Spinelli, D. (1983). Electrophysiological evidence for spatial frequency selective mechanisms in adults and infants. *Vision Research*, *23*(2), 119–127.

Foley, J. M., & Boynton, G. M. (1993). Forward pattern masking and adaptation: effects of duration, interstimulus interval, contrast, and spatial and temporal frequency. *Vision Research*, *33*(7), 959–980.

Foxe, J. J., & Simpson, G. V. (2002). Flow of activation from V1 to frontal cortex in humans: A framework for defining “early” visual processing. *Experimental Brain Research*, *142*(1), 139–150.

Foxe, J. J., Strugstad, E. C., Sehatpour, P., Molholm, S., Pasieka, W., Schroeder, C. E., & McCourt, M. E. (2008). Parvocellular and magnocellular contributions to the initial generators of the visual evoked potential: High-density electrical mapping of the “C1” component. *Brain Topography*, *21*(1), 11–21.

Gardner, J. L., Sun, P., Waggoner, R. A., Ueno, K., Tanaka, K., & Cheng, K. (2005). Contrast adaptation and representation in human early visual cortex. *Neuron*, *47*(4), 607–620.

Goldstone, R. L. (1998). PERCEPTUAL LEARNING. *Annul Review of Psychology, 49,* 585-612.

Gomez-Gonzalez, C. M., Clark, V. P., Fan, S., Luck, S. J., & Hillyard, S. A. (1994). Sources of attention-sensitive visual event-related potentials. *Brain Topography*, *7*(1), 41–51.

Greenlee, M. W., Georgeson, M. A., Magnussen, S., & Harris, J. P. (1991). The time course of adaptation to spatial contrast. *Vision Research*, *31*(2), 223–236.

Greenlee, M. W., & Heitger, F. (1988). The functional role of contrast adaptation. *Vision Research*, *28*(7), 791–797.

Greenlee, M. W., & Magnussen, S. (1988). Interactions among spatial frequency and orientation channels adapted concurrently. *Vision Research*, *28*(12), 1303–1310.

Grill-Spector, K., Henson, R., & Martin, A. (2006). Repetition and the brain: neural models of stimulus-specific effects. *Trends in Cognitive Sciences*, *10*(1), 14–23.

Grootswagers, T., Wardle, S. G., & Carlson, T. A. (2017). Decoding Dynamic Brain Patterns from Evoked Responses: A Tutorial on Multivariate Pattern Analysis Applied to Time Series Neuroimaging Data. *Journal of Cognitive Neuroscience*, *29*(4), 677–697.

Haak, K. V, Fast, E., Bao, M., Lee, M., & Engel, S. A. (2014). Four days of visual contrast deprivation reveals limits of neuronal adaptation. *Current Biology*, *24*(21), 2575–2579.

Hammett, S. T., Snowden, R. J., & Smith, A. T. (1994). Perceived contrast as a function of adaptation duration. *Vision Research*, *34*(1), 31–40.

Haufe, S., Meinecke, F., Görgen, K., Dähne, S., Haynes, J. D., Blankertz, B., & Bießmann, F. (2014). On the interpretation of weight vectors of linear models in multivariate neuroimaging. *NeuroImage*, *87*, 96–110.

Heinrich, T. S., & Bach, M. (2001). Contrast adaptation in human retina and cortex. *Investigative Ophthalmology and Visual Science*, *42*(11), 2721–2727.

Heinrich, T. S., & Bach, M. (2002a). Contrast adaptation in retinal and cortical evoked potentials: no adaptation to low spatial frequencies. *Visual Neuroscience*, *19*(5), 645–650.

Heinrich, T. S., & Bach, M. (2002b). Contrast adaptation: paradoxical effects when the temporal frequencies of adaptation and test differ. *Visual Neuroscience*, *19*(4), 421–426.

Helwig, N. E. (2018). bigsplines: Smoothing Splines for Large Samples. R package version 1.1-1. https://CRAN.R-project.org/package=bigsplines

Hillyard, S. A., Vogel, E. K., & Luck, S. J. (1998). Sensory gain control (amplification) as a mechanism of selective attention: Electrophysiological and neuroimaging evidence. *Philosophical Transactions of the Royal Society B: Biological Sciences*, *353*(1373), 1257–1270.

Huxlin, K. R. (2008). Perceptual plasticity in damaged adult visual systems. *Vision Research*, *48*(20), 2154–2166.

Jeffreys, D. A., & Axford, J. G. (1972a). Source locations of pattern-specific components of human visual evoked potentials. I. Component of striate cortical origin. *Experimental Brain Research*, *16*(1), 1–21.

Jeffreys, D. A., & Axford, J. G. (1972b). Source locations of pattern-specific components of human visual evoked potentials. II. Component of extrastriate cortical origin. *Experimental Brain Research*, *16*(1), 22–40.

Kelly, S. P., Gomez-Ramirez, M., & Foxe, J. J. (2008). Spatial attention modulates initial afferent activity in human primary visual cortex. *Cerebral Cortex*, *18*(11), 2629–2636.

Kleiner, M., Brainard, D., & Pelli, D. (2007). "What's new in Psychtoolbox-3?" *Perception, 36,* ECVP Abstract Supplement.

Kohn, A. (2007). Visual adaptation: physiology, mechanisms, and functional benefits. *Journal of Neurophysiology*, *97*(5), 3155–3164.

Krekelberg, B., Boynton, G. M., & van Wezel, R. J. A. (2006). Adaptation: from single cells to BOLD signals. *Trends in Neurosciences*, *29*(5), 250–256.

Kwon, M., Legge, G. E., Fang, F., Cheong, A. M. Y., & He, S. (2009). Adaptive changes in visual cortex following prolonged contrast reduction. *Journal of Vision*, *9*(2), 20.1–16.

Langley, K. (2002). A parametric account of contrast adaptation on contrast perception. *Spatial Vision*, *16*(1), 77–93.

Larsson, J., & Harrison, S. J. (2015). Spatial specificity and inheritance of adaptation in human visual cortex. *Journal of Neurophysiology*, *114*, 1211–1226.

Larsson, J., Landy, M. S., & Heeger, D. J. (2006). Orientation-selective adaptation to first- and second-order patterns in human visual cortex. *Journal of Neurophysiology*, *95*(2), 862–881.

Larsson, J., Solomon, S. G., & Kohn, A. (2016). fMRI adaptation revisited. *Cortex, 80*, 154–160.

Legge, G. E., & Foley, J. M. (1980). Contrast masking in human vision. *Journal of the Optical Society of America*, *70*(12), 1458–1471.

Magnussen, S., & Greenlee, M. W. (1985). Marathon adaptation to spatial contrast: saturation in sight. *Vision Research*, *25*(10), 1409–1411.

Magnussen, S., & Greenlee, M. W. (1986). Contrast threshold elevation following continuous and interrupted adaptation. *Vision Research*, *26*(4), 673–675.

Magnussen, S., & Johnsen, T. (1986). Temporal aspects of spatial adaptation. A study of the tilt aftereffect. *Vision Research*, *26*(4), 661–672.

Mangun, G. R. (1995). Neural mechanisms of visual selective attention. *Psychophysiology*, *32*(1), 4–18.

Mecacci, L., & Spinelli, D. (1976). The effects of spatial frequency adaptation on human evoked potentials. *Vision Research*, *16*(5), 477–479.

Montaser-Kouhsari, L., Landy, M. S., Heeger, D. J., & Larsson, J. (2007). Orientation-Selective Adaptation to Illusory Contours in Human Visual Cortex. *Journal of Neuroscience*, *27*(9), 2186–2195.

Nelson, J. I., Seiple, W. H., Kupersmith, M. J., & Carr, R. E. (1984). A rapid evoked potential index of cortical adaptation. *Electroencephalography and Clinical Neurophysiology*, *59*(6), 454–464.

Norcia, A. M., Gregory Appelbaum, L., Ales, J. M., Cottereau, B. R., & Rossion, B. (2015). The steady-state visual evoked potential in vision research: A review. *Journal of Vision*, *15*(6), 1–46.

Patterson, C. A., Wissig, S. C., & Kohn, A. (2013). Distinct effects of brief and prolonged adaptation on orientation tuning in primary visual cortex. *Journal of Neuroscience*, *33*(2), 532–543.

Pavan, A., Marotti, R. B., & Campana, G. (2012). The temporal course of recovery from brief (sub-second) adaptations to spatial contrast. *Vision Research*, *62*, 116–124.

Pelli, D. G. (1997). The VideoToolbox software for visual psychophysics: Transforming numbers into movies. *Spatial Vision, 10*, 437–442.

Proverbio, A. M., Del Zotto, M., & Zani, A. (2007). Inter-individual differences in the polarity of early visual responses and attention effects. *Neuroscience Letters*, *419*(2), 131–136.

R Core Team (2019). R: A language and environment for statistical computing. R Foundation for Statistical Computing, Vienna, Austria. URL https://www.R-project.org/

Rebaï, M., & Bonnet, C. (1989). Visual adaptation to a spatial contrast enhances visual evoked potentials. *Perception & Psychophysics*, *46*(6), 537–545.

Regan, D. (1983). Spatial frequency mechanisms in human vision investigated by evoked potential recording. *Vision Research*, *23*(12), 1401–1407.

Ross, J., & Speed, H. D. (1996). Perceived contrast following adaptation to gratings of different orientations. *Vision Research*, *36*(12), 1811–1818.

Sagi, D. (2011). Perceptual learning in Vision Research. *Vision Research, 51*, 1552–1566.

Sclar, G., Lennie, P., & DePriest, D. D. (1989). Contrast adaptation in striate cortex of macaque. *Vision Research*, *29*(7), 747–755.

Seitz, A. R., & Dinse, H. R. (2007). A common framework for perceptual learning. *Current Opinion in Neurobiology, 17*, 148–153.

Sharpee, T., Sugihara, H., Kurgansky, A. V, Rebrik, S. P., Stryker, M. P., & Miller, K. D. (2006). Adaptive filtering enhances information transmission in visual cortex. *Nature*, *439*(7079), 936–942.

Snippe, H. P., & van Hateren, J. H. (2003). Recovery from contrast adaptation matches ideal-observer predictions. *Journal of the Optical Society of America A*, *20*(7), 1321–1330.

Solomon, S. G., & Kohn, A. (2014). Moving sensory adaptation beyond suppressive effects in single neurons. *Current Biology*, *24*(20), 1012-1022.

Srinivasan, M. V., Laughlin, S. B., & Dubs, A. (1982). Predictive coding: A fresh view of inhibition in the retina. *Proceedings of the Royal Society of London B: Biological Sciences, 216*, 427–459.

Stecher, S., Sigel, C., & Lange, R. V. (1973). Spatial frequency channels in human vision and the threshold for adaptation. *Vision Research*, *13*(9), 1691–1700.

Suter, S., Armstrong, C. A., Suter, P. S., & Powers, J. C. (1991). Spatial-frequency-tuned attenuation and enhancement of the steady-state VEP by grating adaptation. *Vision Research*, *31*(7–8), 1167–1175.

Tootell, R. B., Hadjikhani, N. K., Vanduffel, W., Liu, a K., Mendola, J. D., Sereno, M. I., & Dale, a M. (1998). Functional analysis of primary visual cortex (V1) in humans. *Proceedings of the National Academy of Sciences of the United States of America*, *95*(3), 811–817.

Villeda, S. A., Plambeck, K. E., Middeldorp, J., Castellano, J. M., Mosher, K. I., Luo, J., … Wyss-Coray, T. (2014). Young blood reverses age-related impairments in cognitive function and synaptic plasticity in mice. *Nature Medicine*, *20*(6), 659–663.

Wark, B., Fairhall, A., & Rieke, F. (2009). Timescales of inference in visual adaptation. *Neuron*, *61*(5), 750–761.

Wainwright, M. J. (1999). Visual adaptation as optimal information transmission. *Vision Research*, *39*, 3960–3974.

Webster, M. A. (2011). Adaptation and visual coding. *Journal of Vision*, *11*(5), 1–23.

Webster, M. A. (2012). Evolving concepts of sensory adaptation. *F1000 Biology Reports*, *4*(November), 21.

Wyss-Coray, T. (2016). Ageing, neurodegeneration and brain rejuvenation. *Nature, 539,* 180–186.

Zani, A., & Proverbio, A. M. (1997). Attention modulation of C1 and P1 components of visual evoked potentials. *Electroencephalography and Clinical Neurophysiology. 103*, 15–3, 97.

Zhang, P., Bao, M., Kwon, M., He, S., & Engel, S. A. (2009). Effects of Orientation-Specific Visual Deprivation Induced with Altered Reality. *Current Biology*, *19*(22), 1956–1960.